Annu. Rev. Fluid Mech. 2004. 36:381–411
doi: 10.1146/annurev.fluid.36.050802.122124

ENGINEERING FLOWS IN SMALL DEVICES: Microfluidics Toward a Lab-on-a-Chip

H.A. Stone,[1] A.D. Stroock,[2] and A. Ajdari[3]
[1]*Division of Engineering and Applied Sciences, Harvard University, Cambridge, Massachusetts 02138; email: has@deas.harvard.edu*
[2]*School of Chemical and Biomolecular Engineering, Cornell University, Ithaca, New York 14853; email: ads10@cornell.edu*
[3]*Physico-Chimie Théorique, UMR CNRS-ESPCI 7083, ESPCI, 10 rue Vauquelin, 75005 Paris, France; email: armand@turner.pct.espci.fr*

Key Words low-Reynolds-number hydrodynamics, electro-osmosis, nanofluidics, microdevices, mixing

■ **Abstract** Microfluidic devices for manipulating fluids are widespread and finding uses in many scientific and industrial contexts. Their design often requires unusual geometries and the interplay of multiple physical effects such as pressure gradients, electrokinetics, and capillarity. These circumstances lead to interesting variants of well-studied fluid dynamical problems and some new fluid responses. We provide an overview of flows in microdevices with focus on electrokinetics, mixing and dispersion, and multiphase flows. We highlight topics important for the description of the fluid dynamics: driving forces, geometry, and the chemical characteristics of surfaces.

1. INTRODUCTION

Microfluidics refers to devices and methods for controlling and manipulating fluid flows with length scales less than a millimeter. Studies of such fluid-related phenomena have long been part of the fluid mechanical component of colloid science (e.g., Russel et al. 1989) and plant biology (Canny 1977) and draw on many classical features of the dynamics of viscous flows (e.g., Happel & Brenner 1965, Batchelor 1977). However, the subject has received enormous recent attention because of (*a*) the availability of methods for fabricating individual and integrated flow configurations with length scales on the order of tens and hundreds of microns and smaller (e.g., Ho & Tai 1998, Stone & Kim 2001, Whitesides & Stroock 2001), (*b*) rapid developments in biology and biotechnology for which manipulations on the cellular length scale (and below) and the ability to detect small quantities and manipulate very small volumes (typically less than 1 microliter) offer advantages (Voldman et al. 1999, Jain 2000, Beebe et al. 2002), (*c*) the quest for cheap portable devices able to perform simple analytical tasks, and (*d*) the potential use of

microsystems to perform fundamental studies of physical, chemical, and biological processes. This trend is continuing; moreover, the term nanofluidics emphasizes the desire to manipulate flows on the scale of DNA strands, other biopolymers, and large proteins.

There are many journals now reporting applications at the micron scale, though they may not be familiar to fluid dynamicists (e.g., *Lab-on-a-Chip*, *Sensors and Actuators*, and *Analytical Chemistry*). Indeed, the microfluidics literature contains descriptions of many kinds of functional elements including valves, pumps, actuators, switches, sensors, dispensers, mixers, filters, separators, heaters, etc., some of which may motivate investigations of new flow configurations (e.g., Gad-el-Hak 2001). The lab-on-a-chip concept, illustrated in Figure 1*a* (Burns et al. 1998), indicates the goal to fully integrate these components so as to succeed with chemical synthesis, analysis (e.g., characterization, identification, and separation), reactions, and so on using only very small fluid volumes. In many applications a valuable feature of microflows is that the dynamics in a single channel can be replicated in many channels, which can be organized into subnetworks and controlled as indicated in Figure 1*b* (e.g., Thorsen et al. 2002).

In this article we highlight recent microfluidic research trends with emphasis on topics of fundamental interest for understanding fluid motion and associated transport processes. In a few places we draw examples from our own work, but we try to provide a broad perspective and give the reader references to related studies. We focus our attention on liquid flows, and do not discuss themes essential for analytical or preparative purposes such as chemical labeling and detection, specific separation processes, etc. (e.g., Reyes et al. 2002, Auroux et al. 2002). We also leave aside a discussion of the variety of methods for making microdevices (e.g., see Madou 1997, Kovacs 1998, Quake & Scherer 2000, Ng et al. 2002), and only mention that most techniques produce planar structures with long and narrow channels for which lubrication-style analyses are often appropriate.

We subdivide the discussion into three primary areas: electrokinetics, which we discuss in Section 2; mixing and dispersion, which we discuss in Section 3; and multiphase flows, which we discuss in Section 4. In all cases, flows can be described by a continuum approach, and in these small systems special attention has to be given to surface effects and geometrical features. For the engineer and scientist, the basic paradigm is one of "scale down" rather than the more familiar "scale up," but the role of dimensional analysis as a guide remains the same. In particular, the most important issues are not "macro" versus "micro" but rather the relative magnitude of various effects as characterized traditionally using dimensionless parameters.

1.1. Manipulating Microflows

Microfluidic flows are readily manipulated using many kinds of external fields (pressure, electric, magnetic, capillary, and so on). As dimensions shrink, the

TABLE 1 Forces and external fields with which to manipulate flows in microfluidic configurations. It is also possible to use external means to manipulate particles embedded in flows, as in electrophoresis or the use of magnetic forces (e.g., Zabow et al. 2002)

Driving force	Subcategorization	Remarks; representative references
Pressure gradient ∇p		Familiar case as in pipe flow
Capillary effects	Surface tension, γ	Capillary pressure difference
	Thermal	(e.g., Sammarco & Burns 1999)
	Electrical (electrocapillarity)	(e.g., Pollack et al. 2000; Prins et al. 2001)
	Surface tension gradients, $\nabla\gamma$	Typically involve thin films
	Chemical	(e.g., Gallardo et al. 1999)
	Thermal	(e.g., Kataoka & Troian 1999)
	Electrical	
	Optical	Photoresponsive materials
Electric fields **E**	DC electro-osmosis	Uniform velocity field
	AC electro-osmosis	Rectified flows
	Dielectrophoresis	Response $\propto \nabla \mathbf{E}^2$
Magnetic field/ Lorentz forces	Magnetohydrodynamic stirring	(e.g., Bau et al. 2001)
Rotation	Centrifugal forces	(e.g., R.D. Johnson et al. 2001)
Sound	Acoustic streaming	

relative importance of surface to volume forces increases. Such manipulations of flow can be achieved either by forces applied macroscopically, e.g., at appropriate inlets and outlets, or can be generated locally within the microchannel by integrated components. Table 1 summarizes frequently mentioned driving forces for controlling microflows.

For example, when a gas-liquid or liquid-liquid interface is present, fluid motion can be generated by controlling spatial variations of surface tension (so-called Marangoni stresses). These variations can be created with thermal, chemical, electrical, or light gradients. It is also possible to move liquid/gas or liquid/liquid meniscii in channels with partially wetting surfaces by using capillary pressure gradients. Following the Young-Laplace law, the latter can be generated by varying along the channel either wetting properties (contact angle, surface tension) by one of the above mentioned means, or geometrical features (channel diameter). For example, thermal gradients can give capillary pressure motion of droplets (e.g., Sammarco & Burns 1999), whereas variation of channel width allows liquid motion within a channel without a power supply (Juncker et al. 2002).

Alternatively, electrokinetics is now studied in a variety of forms for controlling microflows. Electro-osmosis, where the fluid moves relative to stationary charged boundaries; dielectrophoresis, which moves an interface (often a particle) in a gradient of electric field; and electrowetting, where the electric field modifies

wetting properties, have all been exploited. AC and DC fields can be considered, and the system response then depends on frequency and amplitude of the field. Both capillary-driven and electrically driven flows offer advantages relative to the more familiar pressure-driven flows as the device scale is reduced, though both may be hindered, or potentially even eliminated, by significant surface contamination or heterogeneities.

Other means can be used to control flows. In particular, external fields can be used to induce motion of objects embedded in the fluid, or the channel walls can be systematically distorted: magnetic fields can influence flows directly or manipulate dispersed magnetic particles, sound fields can produce acoustic streaming motions, cyclic deformation of a wall can induce peristaltic pumping, etc.

For each manner of driving a fluid motion, the surface characteristics of the device can also be exploited to provide additional control. For example, the geometrical, chemical, and mechanical features of the channel and network of channels can be patterned or altered, as summarized in Table 2. In addition, the rheology of the fluid can be significant, so both Newtonian and non-Newtonian fluids need consideration.

It is then possible to combine the driving forces (Table 1) and the surface characteristics (Table 2) when considering how best to mix, react, detect, analyze, separate, and so on in microflows. A configuration where the driving force and channel characteristics are combined is shown in Figure 2, which illustrates a configuration driven by a pressure gradient, an electric field, or a surface tension gradient $\nabla\gamma$, with the surface modified chemically in stripes (Figure 2*b*) or with the topography modified (Figure 2*c*). These types of couplings can produce three-dimensional flows in simple channel shapes, and so may be useful for mixing flows, for example. Moreover, the chemical variations could also represent changes in wettability and may be used to manipulate the location of an air-water interface in a microflow, such as the pressure-driven flows illustrated in Figure 3 (Zhao et al. 2001).

TABLE 2 Design considerations for controlling flow and transport in a microfluidic channel can include the influence of geometric, chemical, and mechanical characteristics. In addition, electrodes, heaters, piezoelectric actuation, etc. can be embedded in the channel boundaries

Geometry	**Chemical characteristics**	**Mechanical properties**
Network connectivity[a]	Wettability	Hard materials
Channel cross section and curvature[b]	Surface charge	Elastic materials[d]
Surface topography[c]	Chemical affinity	Gels
Porosity (e.g., in packed beds)	Ph/ionic strength sensitivity	Porous materials

[a]Thorsen et al. (2002).

[b]See the discussion of designs of channel cross section for reducing dispersion in Section 3.

[c]Examples are provided in Sections 2 and 3.

[d]For example, see Unger et al. (2000).

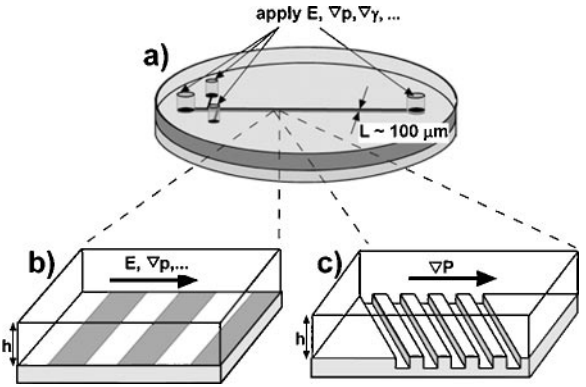

Figure 2 Design considerations for microflows: the driving force for fluid motion (Table 1) and the channel characteristics (Table 2) can be chosen independently, offering potential advantages depending on the desired features of the flow. (*a*) A flow driven by either a pressure gradient, an electric field, or a surface tension gradient. (*b*) A surface modified chemically in stripes. (*c*) A surface modified with topography.

1.2. Experimental Techniques for Flows in Microchannels

For research on microflows, many of the traditional techniques of measuring fluid behavior have been adapted or replaced due to the small size and the planar format of these systems. For example, integrated probes, such as shear stress sensors and thermal anemometers, have been developed for measuring gas and liquid flows in microsystems (Tai & Muller 1988, Liu et al. 1994). The integration of the probe directly into the device is attractive because it may facilitate closed-loop control of flows in devices that include both microfluidic and microelectronic elements.

Most other measurements of microflows have been performed with optical microscopes. An adaptation of particle image velocimetry (PIV) known as micro-PIV can yield a spatial resolution of the flow field of approximately one micron (Santiago et al. 1998). Fluorescence microscopy has also been used to observe microflows. In one variant, a spatially localized pulse from a high-intensity laser is used to generate a fluorophor photochemically in a small volume of fluid in the channel. The advection of this fluorescent volume is observed by fluorescence microscopy in order to visualize the flow profile and speed of the flow (Paul et al. 1998). Confocal fluorescence microscopy has also been used to observe the three-dimensional structure of steady flows in microchannels (Knight et al. 1998, Ismagilov et al. 2000); an example is provided in Section 3.2. In general, there remain opportunities for new developments in the visualization of microflows.

1.3. Fluid Mechanics of Microdevices

A few elementary remarks about fluid mechanics are in order. The typical microchannel is manufactured using planar lithographic techniques (e.g., Kovacs

1998), has a rectangular cross section, and the working fluid is most often water. In some cases, rounding of corners can occur, which may significantly impact dispersion. Moreover, efficient utilization of chip real estate can require curved, zig-zag, or spiral-shaped channels. Three-dimensional configurations have been made and are likely an area for future developments (e.g., Liu et al. 2000). Although steady operating conditions are often maintained, cyclic motions such as peristalsis and rectified effects such as AC electro-osmosis (e.g., Ajdari 2000) or acoustic streaming are possible.

In a wide variety of circumstances the Reynolds number is small (often on the order of unity or smaller) or at least not so large that the convective terms of the Navier-Stokes equations are important. For example, in a channel with height 100 microns, a flow with water (shear viscosity $\mu \approx 0.01$ gm/cm $\cdot$ sec) at a typical speed 1 cm/sec has a Reynolds number of unity. Laminar flow should be expected in the usual case and because the channel width and height are generally much less than its length, lubrication theory is often very useful. Even increasing the flow speed a factor of 100 will not necessarily alter this basic description in simple geometries. Consequently, typical velocity profiles in simple geometries are parabolic in pressure-driven situations, nearly uniform for electro-osmotic flows (EOFs), or a superposition of both in a general situation. Because of the low value of the Reynolds number, turbulence, though not impossible, is uncommon with the consequence that mixing is difficult. Even where an effect of turbulence may have been produced, it should vanish upon further scaling down.

Flows can therefore usually be described by Stokes equations for incompressible motions with no-slip boundary conditions, and classical results are often useful. For example, in a rectangular channel of height h and width w, the pressure drop Δp over a length L is related to the volumetric flow rate Q by $Q = \frac{wh^3 \Delta p}{12\,\mu L}\,[1 - O(h/w)]$, where the approximate form $O(h/w) = \frac{6(2^5)}{\pi^5}\frac{h}{w}$ gives less than 10% error for $h/w \leq 0.7$. The scaling with $h^3 w$ demonstrates the significant impact of changes in the smallest dimensions. Nevertheless, new analyses are necessary as three-dimensional geometries (e.g., turns, surface corrugations, etc.) lead to new questions regarding the detailed flow and associated transport properties. As many of the examples in this article indicate, the flows often involve multiple physical effects, so it is not generally a simple matter to produce closed-form expressions for the detailed flow field.

There are also situations where it is necessary to proceed (usually with care) beyond the simple framework just described. Here we provide three examples where the flow is impacted by a finite Reynolds number, a finite compressibility, and a finite amount of slip, respectively.

1.3.1. REVERSIBILITY AND PERIODIC FLOWS IN CONVERGING/DIVERGING GEOMETRIES

Consider an asymmetric converging-diverging channel along which an oscillatory pressure is applied. Olsson et al. (1996) showed that a device with dimensions $h \times w \times \ell \approx 50 \times 100 \times 10^3\ \mu$m generates a net flow over every cycle of pressure. This response requires inertial effects as zero Reynolds–number flows are

kinematically reversible (e.g., Leal 1992). If U denotes the maximum velocity during a cycle, the appropriate Reynolds number for a steady flow in this configuration (as is familiar from lubrication theory) is $\mathcal{R} = \rho U h^2/\mu\ell$, which is a factor of h/ℓ smaller than the common estimate $\rho U h/\mu$ (e.g., Leal 1992). For the experimental results referenced above, $\mathcal{R} = O(1)$ or smaller, rather than the values $\rho U h/\mu = O(10\text{–}100)$ reported. Consequently, scaling this device down to smaller dimensions should dramatically decrease its pumping efficiency. Similar statements hold for the so-called Tesla valve (e.g., Forster et al. 1995), which cannot display asymmetric flow rate/pressure drop characteristics as the Reynolds number decreases toward zero, in contrast to existing suggestions. High-frequency (ω) motions can impact the response, but only when $\rho\omega h^2/\mu > O(1)$, which requires frequencies greater than 1000 Hz for conditions indicated here.

1.3.2. A SURPRISINGLY LONG TRANSIENT [For an example, see Tabeling (2001), who refers to a private communication from Ulmane & Ho (unpublished data) and Martin et al. (1975)]. A common way to produce flow in a microdevice is to use a syringe pump. We model the latter by a large rigid rectangular channel ($H \times W \times L$ with $H = O(W) < L$) and the former by a narrow channel ($h \times w \times \ell$, with $h = O(w) < \ell$) with heights $h \ll H$, so that the global steady resistance to flow is controlled by the smaller channel: the imposed flow rate Q then requires the pressure drop $\Delta p = O(\mu\ell Q/h^3 w)$. However, to establish this value of Δp, it is necessary to initially compress the flow in the larger chamber, which involves the elasticity (i.e., compressibility) of the liquid (not sound waves or vorticity diffusion)! Denoting the Young's modulus for the liquid as E, this compression time τ is estimated from $\Delta p = E\cdot(Q\tau/HWL)$, or $\tau = O(\mu HWL\ell)/(h^3 wE)$, which can be minutes or even longer for micron-scale systems. In some situations, small bubbles in inlet tubes can seriously affect the transient time. Also, the transient time for displacement-driven and pressure-driven flows can be impacted by the elasticity of boundaries (e.g., those fabricated using soft-lithography).

1.3.3. SLIP BOUNDARY CONDITIONS The ability to probe small length scales and to chemically pattern surfaces to make them solvophobic has revived the question of the applicability of no-slip boundary conditions even for small molecule liquids (e.g., Vinogradova 1999, Cottin-Bizonne et al. 2002, Lauga & Stone 2003). Three kinds of experiments have been performed to probe this issue: (*1*) measurement of pressure-driven flow rates in circular tubes and rectangular channels, (*2*) force versus speed measurements for squeeze flows in the surface forces apparatus and similar devices, and (*3*) direct observation of the flow in the vicinity of an interface (by PIV or evanescent wave techniques). Most measurements are used to infer an effective slip length b for a mixed boundary condition ($\mathbf{u} - b\partial_n\mathbf{u} = \mathbf{0}$ along the liquid-solid surface, where ∂_n denotes the derivative normal to the boundary). Several tentative conclusions can be drawn: (*a*) no-slip conditions apply for almost all experiments with fluids that wet boundaries (e.g., Sharp et al. 2001; see, however, Pit et al. 2000 and Choi et al. 2002); (*b*) a small amount of roughness on an otherwise slip surface produces an effective no-slip boundary condition (Richardson

1973, Jansons 1988, Zhu & Granick 2002); (*c*) some experiments with partially wetting fluids produce results consistent with a slip boundary condition, possibly because of gas or vapor cavities or films along the boundary; this effect, and also adhesion, may be purposefully enhanced by a "spiky" roughness at small scales (e.g., Kim & Kim 2002, Cottin-Bizonne et al. 2003). In conclusion, except for special circumstances requiring care and clever design, the no-slip boundary conditions remains an excellent approximation for flows at scales above tens of nanometers.

2. ELECTRO-OSMOTIC FLOWS AND ELECTROKINETIC EFFECTS IN MICROSYSTEMS

2.1. Electrokinetic Phenomena

Electrokinetics refers to the coupling between electric currents and fluid flow in liquids containing electrolytes. These bulk effects are often generated within the Debye screening layer that forms at charged interfaces. Many excellent references are available for colloidal and porous systems, e.g., Saville (1977), Russel et al. (1989), and Probstein (1994).

When the walls bounding the liquid are charged, there are two primary electrohydrodynamic phenomena: (*a*) electro-osmosis, where an electric field applied along a liquid-filled channel generates a flow, and (*b*) streaming current and streaming potential, where a pressure-driven flow drags ions tangential to the surface and thereby generates an electric current. This current can either be collected through an electric short-circuit, or recirculates within the electrolyte channel by conductivity, in which case a steady-state electric potential difference can be measured between the ends of the channel. The same couplings occur at the interface between an immersed charged (colloidal) object and the liquid: electrophoresis, where a field generates motion of the object relative to the fluid; sedimentation potential, where a vertical potential difference appears in a sedimenting system; and various electroviscous effects, where the flow-induced distortion of the Debye layer affects the static and dynamic properties of a suspension.

We focus primarily on EOFs, and the electric generation and control of flows in microsystems. Elementary cases, where effects are linear in the applied field, are considered first, after which other relevant but more complex situations are discussed.

2.2. Electro-Osmosis: The Basic Phenomenon

When an electrolyte is adjacent to a surface, the chemical state of the surface is generally altered, either by ionization of covalently bound surface groups or by ion adsorption. The net effect is that the surface inherits a charge while counterions are released into the liquid (e.g., common glass, SiOH, in the presence of water, ionizes to produce charged surface groups SiO^-, and releases a proton). At equilibrium, a balance between electrostatic interactions and thermal agitation

generates a charge density profile: the liquid is electrically neutral but for a charged layer adjacent to the boundary, which bears a charge locally equal in amplitude and opposite in sign to the bound charge on the surface. The characteristic thickness of this Debye layer, λ_D, decreases as the inverse square root of the ion concentration in the bulk of the liquid, and commonly has a magnitude $\lambda_D \approx 1$–100 nm in water.

When an electric field $\mathbf{E}_{ext}$ is applied along a channel, a conductive current and the corresponding local field $\mathbf{E}$ are established throughout the liquid. Typically, the bulk of the liquid remains electrically neutral and so is not acted on by a net force. By contrast, in the Debye layer there is a net electrical charge density, so the local electric field $\mathbf{E}$ that is tangent to the surface of the channel generates a body force on the fluid and thus induces a shear. Consequently, the fluid velocity increases from zero right on the surface (where no slip is assumed) to a finite value $-m_{EO}\mathbf{E}$ at the edge of the thin Debye layer, where m_{EO} is a local mobility characteristic of the surface. The mobility m_{EO} is related to the surface charge density σ_{el}, and when the surface potential is small $m_{EO} = \sigma_{el}\lambda_D/\mu = \zeta\epsilon\epsilon_0/\mu$, where ϵ is the dielectric constant, ϵ_0 is the permittivity of the vacuum, and the "zeta potential" ζ is that of the surface, defined as the location of the no-slip boundary condition. A finite slip length b on the surface increases this mobility by a factor $(1 + b/\lambda_D)$.

In common applications, the double layer is much smaller than any of the macroscopic dimensions (channel widths or heights, or particle dimensions) and so, practically, the liquid appears to slip at the velocity $-m_{EO}\mathbf{E}$ along the surface. This separation of length scales allows a useful simplification whereby the electrohydrodynamic coupling is fully described by this "effective slip" boundary condition, and the resulting bulk liquid motion (electro-osmosis) can then be described using only the Stokes equation. For simplicity we will mostly refer to the "effective slip" description, though refinements are sometimes necessary (Anderson 1989), e.g., at very low ionic strengths or for submicron channels (see Ramsey et al. 2002 and Section 2.6).

The magnitude of velocities in EOF are set by the effective slip phenomenon and are independent of the dimensions of the cross section of the channel (if larger than λ_D). Typical surface potentials are of the order of a few tens of millivolts, so that for aqueous systems $m_{EO} \approx 10^{-4}\,\mathrm{cm^2 \cdot s^{-1}\,V^{-1}}$. Consequently, to achieve velocities of a few millimeters per second requires electric fields in the kilovolt per centimeter range. To create the corresponding electrostatic potential drop between the two ends of a centimeter-long channel thus requires a high-voltage supply, which is an obvious impediment to their use in portable devices.

2.3. Electro-Osmotic Flows in Homogeneous and Heterogeneous Channels

Standard fabrication methods for microsystems yield chemically and electrically homogeneous surfaces, and thus a homogeneous surface electrical mobility m_{EO}. Then, there is a remarkable mapping of the electro-osmotic velocity field $\mathbf{u}(\mathbf{x})$ on to the local electric field $\mathbf{E}(\mathbf{x})$. Indeed, the latter obeys Laplace's equation

($\nabla^2\mathbf{E} = \mathbf{0}$), so that a solution to the bulk hydrodynamic problem (Stokes equation, $\mathbf{0} = -\nabla p + \mu\nabla^2\mathbf{u}$) that satisfies the effective slip condition corresponds to no pressure gradient and a potential flow $\mathbf{u}(\mathbf{x}) = -m_{EO}\mathbf{E}(\mathbf{x})$ everywhere. In a straight homogeneous capillary, an axially applied electric field $\mathbf{E}_{ext}$ is constant and generates a uniform "plug-like" EOF $\mathbf{u}(\mathbf{x}) = -m_{EO}\mathbf{E}_{ext}$.

Mapping the flow field onto the applied electric field requires the compatibility of the boundary conditions at the extremities of the channel. For example, the plug flow mentioned above implies pressure equality between the two ends where liquid can freely flow in and out. If the flow rate is constrained at the ends of the channel, then a pressure drop builds up so as to recirculate part of the fluid through the channel. The overall EOF is then the superposition of the plug flow and a recirculation parabolic Poiseuille profile (Anderson & Idol 1985, Herr et al. 2000, Long et al. 1999).

In practice, electrical heterogeneities can occur either accidentally because of defects in the surface treatment, or by adsorption of some chemical species (e.g., Ghosal 2003), or could be purposefully designed by the controlled distribution of surface charge on the walls of the channels. The potential importance of the effects of heterogeneous distributions of surface charge on electrokinetic phenomena have been recognized in theoretical studies (Anderson 1985 for electrophoresis and Anderson & Idol 1985 for electro-osmosis). When an electric current runs through a heterogeneous channel, the electrical mobility m_{EO}, and thus the effective slip velocity, varies along the channel, triggering pressure gradients and nonuniform flows, such as recirculating rolls and multidirectional flows, within the bulk (Ajdari 1995, Herr et al. 2000, Stroock et al. 2000). In this way, surface patterns induce patterned bulk flows. Periodic patterns with period $2\pi/q$ on a flat surface generate flow features that penetrate the bulk over a distance $O(q^{-1})$. If, in addition, the surface topography is patterned, it is possible to generate transverse effects within the whole bulk, with, for example, the direct electro-osmotic flow at some angle to the applied field (Ajdari 1995, 1996). Note that stripes alone, with no topography, even when oriented transverse to the channel axis, yield only the periodic patterns mentioned above. Localized heterogeneities generate long range (algebraically decaying) perturbations of an homogeneous EOF; such features can have potentially substantial effects on hydrodynamic dispersion. The flows due to heterogeneities have been studied theoretically and experimentally, but mostly for one-dimensional geometries, for both abrupt and smooth changes of surface properties (Anderson & Idol 1985, Ghosal 2002, Herr et al. 2000, Keely et al. 1994, Long et al. 1999).

Several experimental studies have demonstrated surface charge control and flow patterning for various EOF applications: adsorption of high molecular weight poly(ions) to generate rolls perpendicular to the field (Stroock et al. 2000; see Figure 4 for the trajectories of tracers) or to modify EOF to reduce dispersion around tight bends in channels (Barker et al. 2000), covalent attachment of ionic species (Smith & Elrassi 1993), light-induced changes of charge density on the surfaces of semiconductors (Moorthy et al. 2001), and application of voltages to

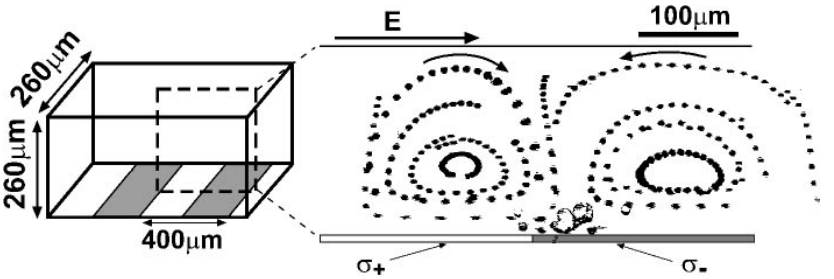

Figure 4 Electro-osmotic flow in the presence of patterned surface charge density (Stroock et al. 2000). The schematic diagram on the left shows a section of a channel in which the base has been patterned with bands of positive (σ_+) and negative (σ_-) surface charge density. The images on the right are a compilation of fluorescence micrographs showing the trajectories of tracer beads in the EOF generated by a steady electric field directed along the channel. The boundaries of the channel are drawn schematically around the image and the direction of the flow is indicated with arrows.

surface-embedded electrodes to switch reversibly the direction of EOF in a portion of a microchannel (Schasfoort et al. 1999).

2.4. Importance of EOF in Microsystems

As with all effects generated at surfaces, electrokinetic influences can be important and useful in microsystems. We emphasize a number of general features: (*a*) EOF can offer significant advantages for driving liquids in miniaturized systems. In a narrow channel of thickness h and width w, for a given potential drop the EOF volume flow rate is proportional to hw, whereas a given pressure drop induces a volume flow rate proportional to h^3w. (*b*) The small cross-sectional area of the fluid-filled channels present high electrical resistance to ionic currents, which allows high electric fields (>100 V/cm) to be maintained with low currents. In addition, ohmic heating is generally limited by the efficient removal of thermal energy in narrow geometries. (*c*) In small systems (<100 microns), spontaneous convection (e.g., thermally driven convection), which obscures electrokinetic motion in large systems, is weak due to viscous damping. (*d*) Items (*b*) and (*c*) favor the use of electrophoresis, which is a powerful means of separation in many analytical microsystems. Nevertheless, electro-osmosis is a natural by-product that should be taken into account and controlled. (*e*) For homogeneous channels, the EOF plug flow allows for the transport of samples without the broadening due to hydrodynamic dispersion present in pressure-driven flows. (*f*) From a technical point of view, some electrokinetic phenomena are more easily studied in the planar format of microfluidic systems due to easier visualization, chemical treatment of surfaces, and integration of electrodes. (*g*) The ability to integrate microelectrodes as part of the channel design permits local generation and control of the electric field, and thus of induced EOFs.

2.5. AC Effects

We have mostly focused on the linear flow response to a steady applied electric field $\mathbf{E}_{ext}$. However, in many cases the applied field will modify the surface charge distribution, and thus m_{EO}, which yields nonlinearities. This effect applies to AC operation, which can be achieved with microelectrodes locally integrated in the microfluidic system. A DC operation in such geometries is often limited by electrochemistry occurring on the electrodes (e.g., irreversible reactions, oxidation, bubble generation due to electrolysis).

The simplest geometry for AC electro-osmosis is possibly that of two flat parallel electrodes on a wall (Gonzàlez et al. 2000, Green et al. 2000). An AC potential applied between the electrodes induces an effective charged surface layer on the electrodes (and thus a contribution m_{AC} to m_{EO}) and a tangential local electric field $\mathbf{E}_t$. Using the effective slip description, the flow response then shows a rectified net steady component parallel to the boundaries as the flow is driven by a product of m_{AC} and $\mathbf{E}_t$, both periodic in time, thus producing steady and time-periodic components. For efficient operation, the AC frequency must be chosen within a specific range: it must be low enough for the charged layer to have time to build up partially, but not so high that this build-up is complete, which would screen out the applied field. Similar or related effects induce motion and organization of colloidal particles in a fluid traversed by an AC current (Trau et al. 1996, Yeh et al. 1997, Gong & Marr 2001).

Again, surface control allows design of bulk flows: a given electrode geometry leads to a distribution of the slip velocity, which induces a patterned flow in the bulk of the channel. The periodicity of the electrode pattern imposes the size of the flow features, and counter-rotating rolls can be generated (e.g., Ramos et al. 1998, Ajdari 2000, Nadal et al. 2002, Squires & Bazant 2003). Such flow structures can stir and mix fluid in the vicinity of the electrodes, and can enhance diffusion limited surface/fluid exchanges (e.g., for surface detection purposes).

Micropumps can be fabricated using geometries with a broken symmetry along the channel axis (Ajdari 2000, Brown et al. 2001, Studer et al. 2002, Squires & Bazant 2003). An AC signal on such sets of polar arrays of electrodes generates locally, by AC electro-osmosis, a net pumping through the channel. This approach has potential advantages over the application of pressure or potential drops between the ends of the channel: there is local control, low voltages are used because the electrodes are now only microns apart, and continuous pumping on a circular chromatographic column is possible, increasing its separation capability (Debesset et al. 2002).

2.6. Streaming Potentials

Streaming potential measurements may also be useful in some applications, although they have been less well studied in microsystems. In principle, they can be used either to characterize the flow rate or the surface charge (once the other is known). Similar to electro-osmosis, streaming effects can be understood in a

straightforward manner in the limit of thin Debye layers, and their amplitude is also proportional to the surface electrical mobility m_{EO}. Onsager symmetries exist between electro-osmosis and the streaming effect in both simple homogeneous and complex heterogeneous geometries (Ajdari 2002). In the case of a homogeneous charge density, a pressure drop Δp applied along a straight channel generates a Poiseuille flow that in turn creates a "streaming potential" between its ends $\Delta\phi \approx -(m_{EO}/K)\Delta p$, where K is the electrolyte conductivity, independently of the channel length or cross section. Highly charged surfaces and low ionic strengths give large values of (m_{EO}/K) and thus favor strong effects. The streaming potential in turn induces an EOF that opposes the original Poiseuille flow. This "electroviscous" effect can be significant in narrow channels (Rice & Whitehead 1965), and accounts for the observed 15% increase of the hydrodynamic resistance in a 10-um glass channel for ion concentration less than 10^{-4} molar (Ren et al. 2001).

We close with a note on the significant difficulty of modeling electrokinetic effects in general. Although the effective slip picture in the simple form given above allows a leading-order analysis, a more thorough description is often not possible analytically, in particular for large surface potentials or if surface features have small dimensions comparable to the Debye screening length. If, in turn, the applied electric fields are strong, other effects can become significant: temperature gradients generated by Ohmic heating, consequent conductivity gradients, buildup of charge densities within the bulk, etc. (see Ramos et al. 1998). In addition, an unexplained electrohydrodynamic instability was reported recently (Oddy et al. 2001). Also, if liquids of different ionic strengths (and thus conductivity) coexist within a channel, the description of electrically driven flows gains an additional degree of complexity.

3. MIXING AND DISPERSION

3.1. Goals

An important area in microfluidic research concerns mixing and dispersion of reagents, which can be small molecules, large macromolecules, particles, and bubbles and drops. We discuss three scenarios involving mixing and dispersion. In the first, minimal mixing of solute between adjacent laminar streams is desired, such that a chemical transformation (e.g., deposition onto surfaces) can be performed at specific locations within a channel. Laminar flows are advantageous for this application, because transverse mixing occurs by diffusion alone. In the second, complete and rapid mixing of adjacent laminar streams is desired, as is required for the initiation of a chemical reaction. Simple laminar flows are then a disadvantage, and convective mixing strategies must be developed. In the third, control of axial dispersion of boluses or plugs of miscible solute is desired, such as in applications in which distinct plugs of analytes are transported to a detector. The parabolic profile of pressure-driven flows is a detriment here as the solute is

stretched along the direction of flow; in contrast, the uniform EOF does not suffer this defect.

In most common cases, convective transport is faster than diffusive transport, even though the length scales are small. In other words, the Peclet number, $\mathcal{P} = uh/D_m$, is usually large, where u is the average axial flow speed, D_m is the molecular diffusivity, and h is the typical cross-sectional dimension of the microchannel. Common values of these parameters are $u = 0.1$–1 cm/s, $h = 10^{-3}$–10^{-2} cm, and $D_m = 10^{-7}$–10^{-5} cm^2/sec, where the smaller value corresponds to macromolecules such as proteins. Therefore, $10 < \mathcal{P} < 10^5$.

3.2. Laminar Flow Patterning and Confinement

Laminar flows with high Peclet numbers $\mathcal{P}$ are ideal for the controlled delivery and confinement of reagents. Figure 5 shows a common geometry for this type of experiment, in which two streams of distinct chemical reagents are injected

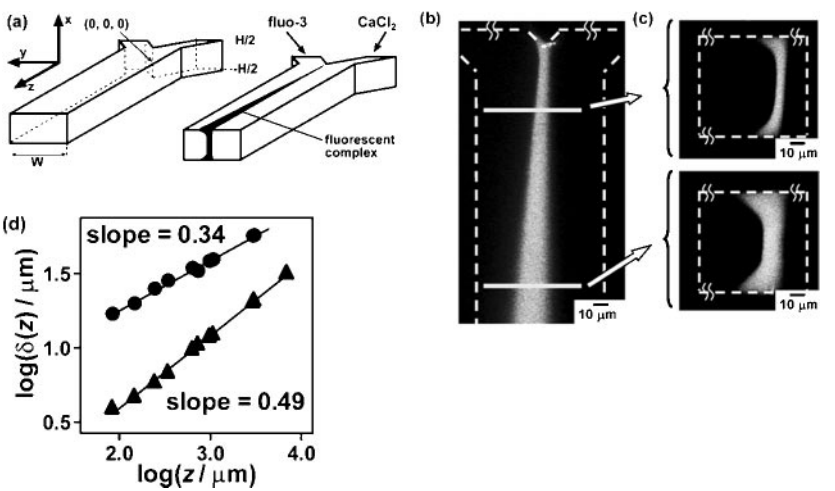

Figure 5 Diffusive mixing between two laminar streams. (*a*) Schematic diagrams of the channel geometry (Ismagilov et al. 2000). The solution on the right contains a calcium-dependent fluorophore, Fluo-3. The solution on the left contains calcium. In water, Fluo-3 and calcium form a fluorescent complex at a diffusion limited rate. (*b*) Fluorescence micrograph that shows a top view of a channel as in (*a*). The fluorescent intermixed region appears lighter than the background. The right-left asymmetry of the intermixed region arises because calcium diffuses more rapidly than Fluo-3. (*c*) Confocal fluorescence micrographs of two vertical cross sections of the channel. (*d*) Experimentally measured scaling of the width of the diffusively mixed region as a function of the axial distance down the channel. The circles represent values measured in the center of the channel ($x = 0$), and the triangles represent values measured near the bottom wall ($x = -H/2$).

side-by-side into a single microchannel. The streams mix only by diffusion across their common interface so we address transverse diffusive transport in Poiseuille flow.

Consider pressure-driven laminar flow of two adjacent miscible streams in a straight channel (Figure 5), with z denoting the flow direction. The interfacial region, of thickness δ_y, thickens owing to molecular diffusion. Away from boundaries, the velocity profile is nearly uniform and, as $\delta_y \propto t^{1/2}$, then $\delta_y \propto z^{1/2}$. On the other hand, near boundaries, the velocity varies linearly as a function of distance into the channel (along x as shown in Figure 5). The classical treatment of this problem, given by Lévêque in 1928 (e.g., Stone 1989, Phillips 1990), considers the thickness, δ_x, of the diffusion boundary layer and because by molecular diffusion $\delta_x \propto (D_m t)^{1/2}$, a material element reaches an axial location z after a time $z/(G\delta_x)$, where $G = (\partial u_z/\partial x)$ is the local shear rate. Therefore, $\delta_x \propto (zD_m/G)^{1/3}$. Broadening of concentration distributions in the other transverse direction, along y, also occurs only by diffusion, so the effective scale is set by the shear boundary layer: $\delta_y \propto \delta_x \propto (zD_m/G)^{1/3}$. These concepts have been checked directly using confocal microscopy (Figure 5) (Ismagilov et al. 2000).

The controlled mixing between adjacent laminar streams has been exploited in chemical applications (Knight et al. 1998, Weigl & Yager 1999). For example, in laminar flow patterning, chemical reactions occur at the walls of the microchannel with a spatial resolution that is determined by the thickness, δ_y, at the boundary. This technique was used to fabricate metallic wires (<10 microns wide), which track the local geometry of the channel, by depositing metal from a reaction at the interface between two laminar streams (Kenis et al. 1999). Laminar flow patterning has also been used to deliver multiple reagents to a single living cell with subcellular spatial resolution (Takayama et al. 2001). Finally, the intermixed region between steady laminar flows has been utilized as a reaction vessel in which to perform chemical kinetic studies. Temporal resolution can be achieved by observing the state of the reaction at different axial positions along the channel because distance in the flow direction translates into a time for reaction (Knight et al. 1998, Pollack et al. 1999); see also the mixing application with small drops in Section 4.2.

3.3. Enhancing Mixing

Mixing between the adjacent laminar streams in a straight, smooth-walled microchannel occurs only by diffusion, and the axial distance Δz_m required for complete mixing grows linearly with the Peclet number $\mathcal{P}$: $\Delta z_m \approx (h^2/D)u_z = \mathcal{P}h$. Given the typical values stated in Section 3.1, Δz_m can be several meters for a protein solution in a 100 μm-wide channel, which is impractical for a portable system. To decrease the mixing length and mixing time ($t_m = u_z^{-1}\Delta z_m$), transverse flows must be generated, such that solute is transported over the cross section of the channel. There are two general strategies for generating such transverse flows: (*a*) passive methods in which transverse flows result from the interaction of the externally driven flow (e.g., pressure-driven or electro-osmotic) with the fixed

channel geometry, and (*b*) active methods in which transverse flows are generated by oscillatory forcing (mechanical or electrical) within the channel. In all cases, the design of mixers for microchannels has benefited enormously from the literature on laminar mixing (e.g., Aref 1984; Ottino 1989, 1990). Both the concepts of chaotic advection and strategies for generating it are crucial for designing micro-mixers.

3.3.1. PASSIVE MIXERS There are designs for effective macroscopic passive mixers, also known as static mixers, which are generally analyzed for low-Reynolds-number motions (Ottino 1989). It is reasonable to ask if these designs can be miniaturized to serve in microfluidic applications. In general, the answer to this question is no. Two important factors limit the scalability of many macroscopic designs: the first is that the geometrical structures that are common in macroscopic designs of mixers are difficult to microfabricate. For example, this is the case for the Kenics design, a chaotic, laminar, low-Reynolds-number mixer, which includes twisting elements that traverse the cross section of the channel; these blades can not be easily fabricated using layer-by-layer lithographic processes. The second limitation concerns those designs that generate secondary (transverse) flows that are inertial in origin (e.g., the twisted pipe flow analyzed by Jones et al. 1989). Such secondary flows will weaken as the size of the system shrinks because the Reynolds number is expected to decrease. For example, mixing designs based on curved channels, or Dean flows, do not scale down well (Liu et al. 2000). Ideally, micromixers should be designed for Stokes flows.

The challenge in designing passive micromixers is to generate laminar chaos in an accessible geometry. A simple design that satisfies this criterion uses obliquely oriented grooves on one wall of the channel to generate transverse components in steady flows (e.g., Johnson et al. 2002 for EOFs, Stroock et al. 2002a,b for pressure-driven flows). We discuss the origin of this transverse flow for the pressure-driven case in Section 3.4. Figure 6*a*,*b* shows EOF mixing in a grooved channel, where each groove entrains filaments of the two streams, which then mix rapidly by diffusion. Figure 6*c* shows schematically a mixer for pressure-driven flows, in which the grooves form asymmetric herringbones. Secondary flows in the channel cross section alternate along the axial direction and mimic the blinking vortex strategy for chaos in two-dimensional, time-dependent flows (Aref 1984). The sequence of stretches and folds (a baker's transformation) (e.g., see Ottino 1989) that occurs in these flows is such that the interface between unmixed regions grows exponentially with time (or axial distance), and the width of unmixed regions decreases exponentially. This stirring decreases the distance over which diffusion has to act to homogenize the fluid. A consequence of this efficiency is that the mixing length, Δz_m, increases proportional to $\ln \mathcal{P}$ rather than to $\mathcal{P}$ (Figure 6*c*) (for recent ideas for quantifying the mixing process see Meunier & Villermaux 2003). Similar ideas using surface grooves to enhance transport were discussed in the heat transfer literature (Sawyers et al. 1998). Finally, note that though the flow is chaotic, mixing over the cross section may not be uniform (e.g., Kusch & Ottino 1992).

3.3.2. VISCOELASTIC LIQUIDS Another approach to passive mixing involves adding microstructural deformable elements (e.g., macromolecules) to the liquid. Flows of such liquids in curved geometries then generate elastic stresses, which can trigger flow instabilities (Larson et al. 1990, Byars et al. 1994), and the result is a significant enhancement of mixing in a curved channel (Groisman & Steinberg 2001). The onset of this elastic instability occurs above a critical value of $\lambda U \kappa_{str}$, where κ_{str} is the typical curvature of the streamlines, λ is the relaxation time of the solution, and U is the typical flow speed (Pakdel & McKinley 1996, Shaqfeh 1996). Attaining this critical value of $\lambda U \kappa_{str}$ may become difficult as the channel dimensions shrink.

3.3.3. ACTIVE MIXERS Laminar chaos has also been exploited in designs that utilize local forcing within the fluid-carrying system. Variants of the blinking vortex design (Aref 1984, Ottino 1989) have been demonstrated in a planar chamber with flow driven in a source-sink fashion by growth and collapse of bubble-filled chambers (Evans et al. 1997), geometries with transverse flow periodically driven via side channels (e.g., see Tabeling 2001) and magnetohydrodynamic effects (Bau et al. 2001, Yi et al. 2002b). Also, piezoelectric materials allow the generation of traveling waves on the surfaces of microdevices (e.g., Moroney et al. 1991, Miyazaki et al. 1991), and analyses of the flow and potential mixing properties have been reported (e.g., Selverov & Stone 2001, Yi et al. 2002a). Electrokinetic instabilities also produce good mixing flows (Oddy et al. 2001). A challenge in designing active mixers is the choice of driving frequencies and phases, and optimization of such mixers has seldom been addressed.

3.4. Analytical Description of Three-Dimensional Flow in Patterned Channels

We next consider in more detail the role of patterned surface topography for pressure-driven flow in a channel of average height h and width $w \gg h$ (Stroock et al. 2002b, Ajdari 2002) and focus on the main physical and scaling ideas. Electroosmotic flow over obliquely oriented grooves has been studied numerically by Johnson & Locascio (2002), and an analytical treatment of related phenomena can be found in Ajdari (1996, 2002).

In response to a pressure gradient, the principal effect of obliquely oriented surface grooves (Figure 6) is to generate an anisotropic secondary flow in the direction orthogonal to the channel axis. If we consider a Hele-Shaw configuration with grooves of depth $2\alpha h$ ($\alpha \ll 1$) oriented at an angle ϕ relative to the applied pressure gradient, then the average flow (averaged over the period of topography) is an ordinary pressure-driven channel flow with a generalized slip boundary condition at the patterned plane $z = 0$:

$$\mathbf{u} + \alpha^2 h \mathbf{\Lambda} \cdot \frac{\partial \mathbf{u}}{\partial z} = \mathbf{0}, \tag{1}$$

where $\mathbf{\Lambda}$ is a slip tensor characteristic of the surface anisotropy with a functional form that depends on the geometry and orientation of the surface pattern. For example, for straight ridges, the off-diagonal terms of $\mathbf{\Lambda}$ are $(K_\parallel - K_\perp)\sin\phi\cos\phi$, where the terms $\alpha^2 K_\parallel$ and $\alpha^2 K_\perp$ are corrections to the hydrodynamic conductances parallel and perpendicular to the grooves (Stroock et al. 2002b). The solution to channel flow in the lubrication limit is then

$$\mathbf{u} = \frac{1}{2\mu}[(z^2 - h^2)\mathbf{I} - h(z-h)(\mathbf{I} - \alpha^2\mathbf{\Lambda})^{-1}] \cdot \nabla p. \tag{2}$$

For $\alpha^2 \ll 1$, we can write $\mathbf{u} \approx \frac{1}{2\mu} z(z-h)\nabla p - h(z-h)\alpha^2\mathbf{\Lambda} \cdot \nabla p$, where the first term corresponds to a parabolic mean flow and the second term provides a velocity contribution transverse to the main flow with a circulation consistent with a nonzero slip velocity at $z = 0$. In a channel with sidewalls, the transverse slip flow establishes a transverse pressure gradient similar to a lid-driven cavity (Stroock et al. 2002b) (see the inset of Figure 6).

3.5. Controlling Axial Dispersion in Microchannels

Many chemical applications of microfluidic devices would benefit from the ability to limit axial dispersion of miscible solutes within a flow. Efforts to this end have been made for both pressure-driven and EOFs.

3.5.1. PRESSURE-DRIVEN FLOWS The basic concepts of Taylor dispersion in circular capillaries (Taylor 1953) form the basis of all considerations of dispersion in pressure-driven flows. Most microchannels have rectangular, or nearly rectangular, cross sections (height h and width w, with $h < w$ most common). The dispersivity $\mathcal{D}$, or effective diffusivity, differs from the molecular diffusivity D_m in a pressure-driven flow for a perfectly one-dimensional situation ($h/w = 0$) according to $\frac{\mathcal{D}}{\mathcal{D}_m} = 1 + \frac{1}{210}(\frac{Uh}{\mathcal{D}_m})^2$ (compare to $\frac{\mathcal{D}}{\mathcal{D}_m} = 1 + \frac{1}{48}(\frac{Uh}{\mathcal{D}_m})^2$ for a circular section), where U is the average flow speed. Thus, we expect for a channel section with dimensions $h \times w$,

$$\frac{\mathcal{D}}{\mathcal{D}_m} = 1 + \frac{1}{210}\left(\frac{Uh}{\mathcal{D}_m}\right)^2 f\left(\frac{h}{w}, \text{shape}\right), \tag{3}$$

where the function f depends on both the aspect ratio and the detailed cross-sectional shape. One surprise is that in the limit $h/w \to 0$, the dispersivity is predicted to be substantially larger than the ideal one-dimensional result: $\lim_{h/w\to 0} f(h/w) \approx 7.95$ (e.g., Dutta & Leighton 2001). Effectively, slow-moving fluid near the side walls a distance w apart increases the dispersion of a plug of injected solute.

The dispersion may be minimized by profiling the shape of the channel for the same minimum height h and specified width w (Dutta & Leighton 2001). Because slow-moving fluid near the far side walls increases dispersion above the theoretical minimum of an ideal two-dimensional uniaxial flow, then it follows that a channel that is deeper near the side walls produces faster streamlines there

and acts to decrease the dispersion. Of course, such detailed channel shapes may require additional fabrication steps.

Another approach to lowering the axial dispersion is to enhance the rate of transverse exchange between fast- and slow-moving regions relative to pure diffusive transport (the classical Taylor case). Properly designed three-dimensional flows can achieve this reduction; reduced dispersion was demonstrated with the herringbone mixer (Section 3.3) relative to an unmixed flow (Stroock et al. 2002a).

3.5.2. ELECTROKINETICALLY DRIVEN FLOWS—THE IMPACT OF TURNS Electro-osmotic flows in straight channels have uniform velocity distributions in which case the only mechanism for dispersion is molecular diffusion (at least in the absence of adsorption at boundaries). Many designs have turns and these can be a source of dispersion (Culbertson et al. 1998) as bends introduce a difference in path length for fluid elements that move along the inside as compared to the outside of the channel. For a given potential difference, the electric field is higher on the inside of the bend. For a simple turn of angle $\Delta\theta$, centerline radius R, and width w, the convective axial spreading through such a corner is $2w\Delta\theta$, which is independent of the turn radius and the electro-osmotic velocity, and gives the dispersion if diffusion across the channel is slow compared to the transit time through the turn. It is well known that the effective diffusion $\mathcal{D}$ in a shear flow with shear rate G is $\mathcal{D}/D_m = 1 + \frac{1}{30}(Gw^2/D_m)^2$ (e.g., Brenner & Edwards 1993; for the application to turns see Griffiths & Nilson 2000). Because the flow has mean speed $\mu_E E$, the turn introduces a shear $(\mu_E E)/R$ over a time $\tau \approx R\Delta\theta/(\mu_E E)$, and hence in the fast diffusion limit the additional axial dispersive spreading produced by the turn is expected to be approximately $(\mathcal{D}\tau)^{1/2} \approx (\mu_E E w^4 \Delta\theta/(RD_m))^{1/2}$.

One route to decreasing the dispersion is to add a turn of the opposite sense for every turn. Alternatively, the shape of the turn can be manipulated and algorithms for optimization using appropriate cost functions can be utilized (Molho et al. 2001). Experimental studies related to characterizing optimal shapes have also been performed (e.g. Paegel et al. 2000). Alternatively, for spiral channel configurations, the smaller path length of the inner boundary can be compensated for by making the inner boundary wavy (Dutta & Leighton 2002). In addition, patterned surface charge density has been used to compensate for dispersion in corners (TJ Johnson et al. 2001). Most importantly, these studies of minimum dispersion configurations in EOF-driven geometries have introduced optimization strategies into microfluidic design in a manner that includes analysis of the flow, electric field, and so on.

4. MULTIPHASE FLOWS

Flows of gas-liquid or liquid-liquid mixed phases are familiar from many macroscopic systems. The fluid-dynamical response is commonly characterized successfully in terms of the Reynolds and Weber (or capillary) numbers of the flow. When discussing multiphase flows in microdevices there are likewise a myriad of

questions that arise in even simple configurations. For example, it is frequently of interest to determine the size of droplets of the dispersed phase or the speed at which the dispersed phase moves relative to the continuous phase. Also, when two different phases are injected as adjacent streams in one channel, the flow can be stable but, alternatively, one phase can preferentially wet the boundaries and encapsulate the second fluid, either as a continuous stream or discrete drops. In addition, two-phase gas-liquid flows in microdevices can be used to focus columnar liquid samples (e.g., for an application to flow cytometry, see Huh et al. 2002).

In this section we focus on the motion of small liquid droplets in microdevices. Two distinct configurations can be distinguished: drop formation and movement in small channels, which we discuss in Sections 4.2 and 4.3, and drop movements on substrates using micron-scale control of interfacial energies, which we only briefly mention (e.g., Darhuber et al. 2003). A third configuration with some similarities concerns continuous films patterned or controlled using microfluidic steps or micron-scale chemical patterning. In all of these situations, the flows are impacted by interfacial tension and the wetting characteristics of the liquids.

4.1. Fluid Mechanical Preliminaries

The capillary number $\mathcal{C} = \mu u/\gamma$, where γ is the interfacial tension between the two fluid phases, plays an important role in the characterization of these flows. Because $\mu \approx \mu_{H_2O} \approx 10^{-2}$ g/cm/sec, $u \approx 1$–10 cm/sec, and $\gamma \approx 30$ gm/sec^2 when surfactants are present in an aqueous solution ($\gamma \approx 5$ gm/sec^2 at an oil-water interface), then $\mathcal{C} \approx 10^{-3}$–$10^{-2}$. The relative importance of hydrostatic pressure is measured by the Bond number, $\mathcal{B} = \Delta\rho g h^2/\gamma$, where $\Delta\rho$ is the density difference between the phases; for $\Delta\rho = O(1)$ and a 10 micron channel, $\mathcal{B} \approx 10^{-4}$, and is smaller for most liquid-liquid systems, which have a smaller density contrast. In many cases, gravitational effects are small.

Strain rates $\dot{\gamma}$ can be large in the microflows. In the simplest case, $\dot{\gamma} \approx u/h$, which is 10^3–10^4 sec^{-1} for the values given above. Such values are sufficiently large to cause nonNewtonian rheological effects if suspended deformable objects are present. Hence, it is natural to consider the relaxation time τ of suspended drops, macromolecules, or surfactant mesophases, or to consider the time for surfactant adsorption/desorption processes at interfaces, and to organize different systems according to the Deborah number $\dot{\gamma}\tau$. Such systematic studies have not been performed in geometries characteristic of microdevices but there is guidance that can be gained from similar (low-Reynolds-number) studies in macroscopic configurations.

4.2. Drops in Small Devices

Pressure-driven, thermally driven, and electrically driven motions of drops and bubbles are possible. At least three applications of small droplets (or bubbles) can be identified: (*a*) drops as actuators for pumping a primary flow or driving mixing flows, (*b*) drops as individual "chemical reactors," and (*c*) emulsions formation

with a controlled drop size and size distribution. These applications indicate the need to understand drop formation, coalescence, translation, internal mixing, and further drop breakup. Although these problems have been investigated extensively in unbounded flows, and to a certain degree in pipes and channels, much less is known quantitatively about confined systems, which is the case for microfluidics. We next discuss items (*b*) and (*c*) in more detail.

4.2.1. DROPS AS CHEMICAL REACTORS Slugs of liquids can be used to isolate and confine a material or a mixture of materials (e.g., Burns et al. 1996). One advantage of this confinement to a small convecting volume with confined streamlines is that faster mixing of the contents occurs than by diffusion alone, and the transport is accomplished without (axial) dispersion. This approach provides a promising avenue for spatially and temporally resolved chemistry (e.g., Song et al. 2003), which can be used for inexpensive and potentially improved measurements of kinetic and binding constants, as well as measuring aspects of phase and reaction diagrams of multicomponent systems. The sequential formation of small drops, which flow along a microchannel, allows accurate conversion of time variation (e.g., of a chemical reaction) to a steady spatial variation (e.g., along the direction of the flow). Because a drop traveling at 10 cm/sec moves 0.1 cm in 0.01 seconds, and as the entire drop trajectory in a microchannel can be visualized, it is possible to study kinetics with time constants less than 10^{-2} s. However, this time resolution is only possible if internal mixing is achieved quickly relative to the desired temporal resolution. To enhance the rate of mixing inside drops it is necessary to generate time-dependent internal flows, which can be accomplished in pressure-driven flows by using curved channels (Song et al. 2003) or with AC electric fields (e.g., Ward & Homsy 2001).

Figure 7 shows a passive approach to rapid mixing in droplets (Song et al. 2003). Two aqueous streams are mixed inside a droplet formed at a T-junction in a flow of an oil stream, and a fluorescence signal provides a measure of the mixing rate. The fluid motion as a drop moves along the curved channel leads to time-varying internal recirculation that induces efficient mixing. The principles of laminar chaos (e.g., Ottino 1989) may be useful here in designing more efficient mixing protocols.

4.2.2. EMULSIONS IN MICROCHANNELS Liquid-liquid and liquid-gas dispersions are common in macroscopic processes and products of the chemical, health-care, and food industries, so examples of liquid-liquid dispersions abound. Not surprisingly, many studies of emulsification and droplet behavior have been performed in macroscopic, unbounded shear, and extensional flows (Taylor 1934, Rallison 1984, Stone 1994). Recent investigations focused on generating and manipulating emulsions with microfluidic devices are motivated by the potential to use controlled flows and structures on the scale of the droplets to tailor the properties of the emulsions. In particular, it is of interest to control the droplet size and the distribution of sizes. The microchannel geometry takes on added significance

because it can influence the relative rate of rotation to extension in the flow, which is fundamental to break-up processes.

One simple configuration is a T-junction where fluid of one phase flows in one arm and is sheared by a second immiscible phase flowing in the perpendicular arm (Thorsen et al. 2001). Alternatively, it is possible to arrange the two channels in a concentric manner upstream of a small orifice (e.g., Gañán-Calvo & Gordillo 2001), thus creating a strong extensional flow. Figure 8 shows an example of such a microfluidic flow-focusing arrangement for creating a dispersion of water drops in oil (Anna et al. 2003). Here a "phase-like" diagram of the different drop sizes and drop size distributions is shown with the ratio of flow rates (i.e., the volume fraction of the dispersed phase) on the horizontal axis and the continuous phase flow rate (proportional to the capillary number) shown on the vertical axis. In some cases the drop size is effectively set by the size of the orifice designed into the microchannel; in other cases the flow-focusing geometry produces threads that break into drops substantially smaller than the orifice. Other geometries such as extrusion over a step also reproducibly form drops (Sugiura et al. 2001). Finally, it is possible to control the drop size distribution using passive break-up configurations, such as breakup at a T-junction as Figure 9 shows (Link et al. 2003). In particular, small drops can be formed at high dispersed phase volume fractions, which is not achieved by simply forming emulsions at a T-junction or flow-focusing element. Also, breakup into different sized droplets can be accomplished in a controllable manner.

The control of drop breakup in microdevices such as those mentioned above is influenced significantly by surfactants and wetting characteristics. For example, the continuous phase should be the phase that most strongly wets the boundaries. Contact angles and wetting properties depend on the type and concentration of surfactant, and such surfactant effects on drop formation in a T-junction have been investigated experimentally (Dreyfus et al. 2003), but have yet to be analyzed in detail; one example illustrating the effect of surfactants is shown in Figure 8. In addition, because shear rates can be large, new interfacial area is created rapidly (e.g., Figure 8). Thus, the kinetics, and possibly rheology, of surfactants may also play significant roles in the emulsion formation process. Finally, heterogeneities of the solid surface may impact partially wetting situations owing to significant contact line effects.

4.2.3. EXTERNALLY APPLIED FIELDS Other means are available to further control drop sizes. For example, pulsing the pressure field using a piezoelectric sleeve has been used advantageously in improving ink-jet designs for the production of droplets with diameters in the tens of microns range (e.g., Chen & Basaran 2002). Also, electric fields for the formation of jets and sprays is a well-studied area and has been scaled down to a microfluidic device (Schultz et al. 2000). Many future ideas here should be expected.

4.3. Motion of Individual Drops in Microchannels

The experimental results reported in the previous section indicate applications with translation of drops in microchannels. Thus, it is of interest to determine

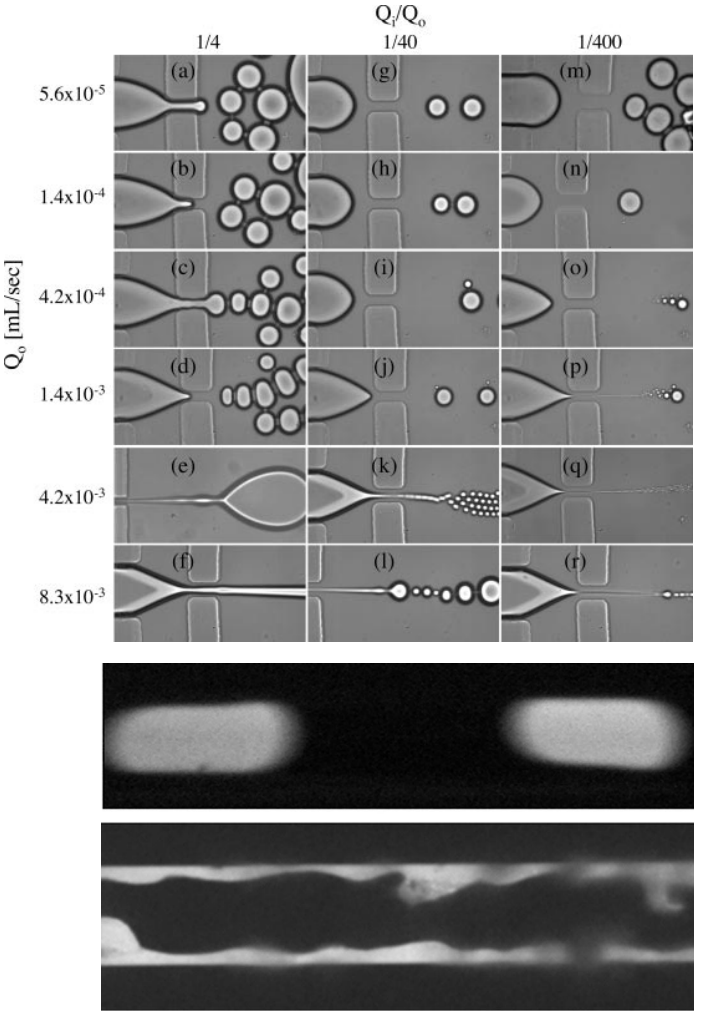

Figure 8 (*Top frame*) Drop formation in a flow-focusing configuration in a microdevice (Anna et al. 2003). Water drops are formed in a silicone oil continuous phase with Span 80 at 0.67 wt% added to the oil phase. The width of the orifice is 43.5 μm, water flows with flow rate Q_i in the central channel of width 197 μm, and oil flows with total flow rate Q_o in the two outer channels of width 278 μm. Each image (*a–r*) shows the typical drop size and size distribution formed at the given flow rate of oil (or capillary number of the continuous phase) and the flow rate ratio or volume fraction of the dispersed phase. [*Middle and bottom frames* (Courtesy of H. Willaime.)] The influence of surfactants on two-phase flow in microchannels. (*top*) Span 80 surfactant at 2.2 weight percent in tetradecane at a flow rate 20 ml/min with the flow rate of water 1 ml/min. Isolated water drops form. (*bottom*) Surfactant-free tetradecane at a flow rate 10 ml/min with the flow rate of water 5 ml/min. Water forms a continuous core.

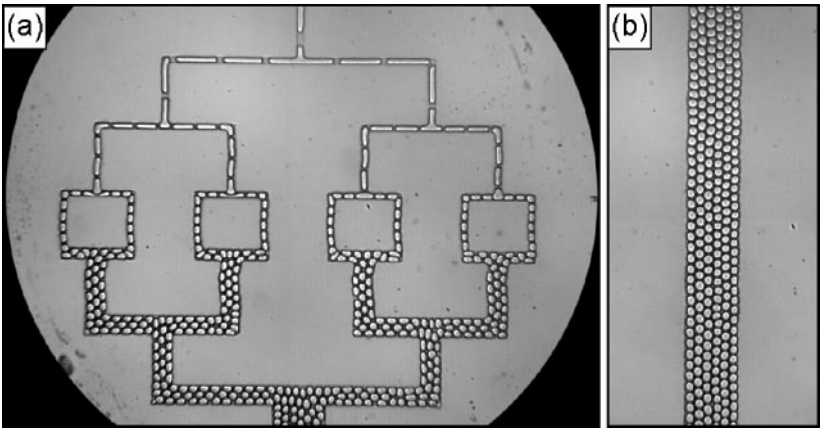

Figure 9 Sequential drop breakup at T-junctions (Link et al. 2003). The ratio of the two daughter droplets can be controlled by changing the lengths of the arms coming off of the T-junction. Generally, it is difficult to form small drops (i.e., of size comparable to or smaller than the channel size) at high-volume fraction of the dispersed phase (e.g., see Figure 8), but with this "passive" route a high-volume fraction is formed initially and then subsequently reduced in size by the extensional breakup at the T-junctions.

the translation speed and the detailed velocity distribution external and internal to the drop. When the drop radius is small compared to the channel dimensions, the drop moves nearly with the local fluid velocity, and corrections for boundary effects and "Faxen" effects based on the pressure-drop across the particle have been studied frequently (e.g., Happel & Brenner 1965). Alternatively, it is common in microfluidic applications for the drop to be close-fitting in the channel.

There are two distinct configurations to consider: a drop separated from the boundaries by a thin wetting film and a drop that forms a distinct contact line with the walls of the channel. In the former case, for a long bubble in pressure-driven flow in a circular capillary, the bubble moves slightly faster than the continuous phase fluid (Bretherton 1961), with a slip velocity proportional to $\mathcal{C}^{2/3}$. Surfactants modify the stress distribution along the interface and produce a small change in the slip velocity (Ratulowski & Chang 1990). In rectangular channels, the thin film separating the drop from the channel is not uniform, and there is extra space in the corners for the liquid to leak past the drop, which then slightly lags the mean flow of the continuous phase (Wong et al. 1995a,b). Also, external fields produce Marangoni stresses that can drive motion; in temperature gradients (Mazouchi & Homsy 2001) drops move toward hotter regions, and electric fields produce electrokinetic effects that move drops (Takhistov et al. 2002). For the case that the two liquids partially wet the channel walls so that the drop makes a finite contact angle, a capillary pressure is responsible for drop translation: thermal (Sammarco

& Burns 1999), electrical (Pollack et al. 2000), and geometric control (Juncker et al. 2002) have been demonstrated.

The ability to manipulate the motion of drops is also of interest for moving drops over surfaces. Again, Marangoni stresses and capillary pressures, which can be manipulated by chemical, thermal, optical, and electrical means, can be useful for microfluidic control; patterned substrates provide an additional avenue of control (e.g., Lee & Laibinis 2000).

5. CONCLUSIONS AND PERSPECTIVES

There are many opportunities for basic and applied contributions in the microfluidics area. One subject that has received little attention has been the study of optimization of different flow configurations (see Section 3.5 for optimization studies for dispersion). Second, because multiple channel characteristics (e.g., geometry, topography, surface treatments) and driving forces can be implemented and combined using straightforward fabrication procedures, it is interesting to think about innovative methods for designing valves, pumps, separation processes, etc. Third, many applications will involve suspended macromolecules, biopolymers, and large shear rates; hence these are conditions where significant changes in the microstructure (e.g., Shrewsbury et al. 2002, Jendrejack et al. 2003) and to the rheology of the fluid are expected. Few microfluidic studies have been reported where the viscoelastic response is important (for an example, see Section 3.3).

As fabrication methods continue to improve, the issue of scaledown will receive more attention. Surface forces then play ever more important roles. To give one example, it is likely that additional aspects of electrokinetics may then need consideration (Section 2 and, in particular, Section 2.6). Nanoscale devices are also becoming more common either by direct nanofabrication or through the engineering of nanocolloidal systems (e.g., porous media, surface nanopatterning, self-assembly of particles) with microfluidic devices. It is less likely that applied pressure gradients are practical and flows will more likely be driven electrokinetically or perhaps by some local forcing mechanism such as peristalsis. Moreover, the Peclet number will then be smaller and mixing may be dominated by simple diffusion. Methods for exploiting this limit, such as Brownian ratchets, will be of interest.

Clearly, there are many interesting fluid mechanics questions that arise with microdevices and many more that remain to be investigated. Although one vision of microfluidics is the "chemical plant on a chip," a more general viewpoint, which encompasses science and applications in cellular biology, material science, chemistry, etc., is to recognize that microfluidic technology offers a synthetic system for controlling transport and chemistry at all length scales below a few millimeters. These systems should provide challenges in fluid dynamics, transport, and engineering design for generations of readers.

ACKNOWLEDGMENTS

We thank S.L. Anna, J. Ashmore, M.P. Brenner, M. Burns, C. Cottin-Bizonne, D. Beebe, R. Ismagilov, T. Jongen and colleagues, I.S. Kang, E. Lauga, D. Leighton, D. Link, L. Locascio, G. McKinley, J.M. Ottino, S. Quake, J. Santiago, D. Saville, T. Squires, P. Tabeling, D. Weitz, and G. Whitesides for helpful conversations and/or correspondence. H.A.S. thanks the National Science Foundation and the Harvard MRSEC (DMR-0213805). H.A.S. thanks J. Magnaudet and the Institut de Mécanique des Fluides in Toulouse for their hospitality during a visit when the first draft of this article was written.

The *Annual Review of Fluid Mechanics* is online at http://fluid.annualreviews.org

LITERATURE CITED

Ajdari A. 1995. Electro-osmosis on inhomogeneously charged surfaces. *Phys. Rev. Lett.* 75:755–58

Ajdari A. 1996. Generation of transverse fluid currents and forces by an electric field: electro-osmosis on charge-modulated and undulated surfaces. *Phys. Rev. E* 53:4996–5005

Ajdari A. 2000. Pumping liquids using asymmetric electrode arrays. *Phys. Rev. E* 61:R45–48

Ajdari A. 2002. Transverse electrokinetic and microfluidic effects in micro-patterned channels: lubrication analysis for slab geometries. *Phys. Rev. E* 65:016301

Anderson JL. 1985. Effect of nonuniform zeta potential on particle movement in electric fields. *J. Colloid Interface Sci.* 105:45–54

Anderson JL. 1989. Colloid transport by interfacial forces. *Annu. Rev. Fluid Mech.* 21:61–99

Anderson JL, Idol WK. 1985. Electroosmosis through pores with nonuniformly charged walls. *Chem. Eng. Commun.* 38:93–106

Anna SL, Bontoux N, Stone HA. 2003. Formation of dispersions using "flow focusing" in microchannels. *Appl. Phys. Lett.* 82:364–66

Aref H. 1984. Stirring by chaotic advection. *J. Fluid Mech.* 143:1–23

Auroux P-A, Iossifidis D, Reyes DR, Manz A. 2002. Micro total analysis systems. 2. Analytical standard operations and applications. *Anal. Chem.* 74:2637–52

Barker SLR, Ross D, Tarlov MJ, Gaitan M, Locascio LE. 2000. Control of flow direction in microfluidic devices with polyelectrolyte multilayers. *Anal. Chem.* 72:5925–29

Batchelor GK. 1977. Developments in microhydrodynamics. In *Theoretical and Applied Mechanics*, ed. W Koiter. pp. 33–55. The Netherlands: Elsevier North Holland

Bau HH, Zhong JH, Yi MQ. 2001. A minute magneto hydrodynamic (MHD) mixer. *Sens. Actuators B* 79:207–15

Beebe DJ, Mensing GA, Walker GM. 2002. Physics and applications of microfluidics in biology. *Annu. Rev. Biomed. Eng.* 4:261–86

Brenner H, Edwards DA. 1993. *Macrotransport Processes*. Boston: Butterworth-Heinemann. 744 pp.

Bretherton FP. 1961. The motion of long bubbles in tubes. *J. Fluid Mech.* 10:166–88

Brown ABD, Smith CG, Rennie AR. 2001. Pumping of water with ac electric fields applied to asymmetric pairs of microelectrodes. *Phys. Rev. E* 63:016305

Burns MA, Johnson BN, Brahmasandra SN, Handique K, Webster JR, et al. 1998. An integrated nanoliter DNA analysis device. *Science* 282:484–87

Burns MA, Mastrangelo CH, Sammarco TS, Man FP, Webster JR, et al. 1996. Microfabricated structures for integrated DNA analysis. *Proc. Natl. Acad. Sci. USA* 93:5556–61

Byars JA, Öztekin A, Brown RA, McKinley GH. 1994. Spiral instabilities in the flow of highly elastic fluids between rotating parallel disks. *J. Fluid Mech.* 271:173–218

Canny MJ. 1977. Flow and transport in plants. *Annu. Rev. Fluid Mech.* 9:275–96

Chen AU, Basaran OA. 2002. A new method for significantly reducing drop radius without reducing nozzle radius in drop-on-demand drop production. *Phys. Fluids* 14:L1–L4

Choi C-H, Westin KJA, Breuer KS. 2002. To slip or not to slip—Water flows in hydrophilic and hydrophobic microchannels. *Pap. 2002-33707, Proc. ASME IMECE, New Orleans, LA*

Cottin-Bizonne C, Barrat J-L, Bocquet L, Charlaix E. 2003. Low friction liquid flows at nanopatterned interfaces. *Nat. Mater.* 2:237–40

Cottin-Bizzone C, Jurine S, Baudry J, Crassous J, Resagno F, Charlaix E. 2002. Nanorheology: An investigation of the boundary condition at hydrophobic and hydrophilic interfaces. *Eur. Phys. J. E* 9:47–53

Culbertson CT, Jacobson SC, Ramsey JM. 1998. Dispersion sources for compact geometries on microchips. *Anal. Chem.* 70: 3781–89

Darhuber AA, Valentino JP, Davis JM, Troian SM. 2003. Microfluidic actuation by modulation of surface stresses. *Appl. Phys. Lett.* 82:657–59

Debesset S, Hayden CJ, Dalton C, Eijkel JCT, Manz A. 2002. A circular AC electroosmotic micropump for chromatographic applications. *Micro TAS*, pp. 655–57

Dreyfus R, Tabeling P, Williams H. 2003. Ordered and disordered patterns in two-phase flow in microchannels. *Phys. Rev. Lett.* 90:144505

Dutta D, Leighton DT Jr. 2001. Dispersion reduction in pressure-driven flow through microetched channels. *Anal. Chem.* 73:504–13

Dutta D, Leighton DT Jr. 2002. A low dispersion geometry for microchip separation devices. *Anal. Chem.* 74:1007–16

Evans J, Liepmann D, Pisano AP. 1997. Planar laminar mixer. *Proc. IEEE 10th Ann. Int. Workshop Micro Electro Mechanical Syst., Nagoya, Jpn.*, pp. 96–101

Forster FK, Bardell RL, Afromowitz MA, Sharma NR, Blanchard A. 1995. Design, fabrication and testing of fixed-valve micropumps. *Proc. ASME Fluids Eng. Div.*, pp. 39–44

Gad-el-Hak M, ed. 2001. *MEMS Handbook*. Boca Raton, FL: CRC Press. 1368 pp.

Gallardo BS, Gupta VK, Eagerton FD, Jong LI, Craig VS, et al. 1999. Electrochemical principles for active control of liquids on submillimeter scales. *Science* 283:57–60

Gañán-Calvo AM, Gordillo JM. 2001. Perfectly monodisperse mirobubbling by capillary flow focusing. *Phys. Rev. Lett.* 87:274501

Ghosal S. 2002. Lubrication theory for electroosmotic flow in a microfluidic channel of slowly varying cross-section and wall charge. *J. Fluid Mech.* 459:103–28

Ghosal S. 2003. The effect of wall interactions in capillary-zone electrophoresis. *J. Fluid Mech.* 491:285–300

Gong T, Marr WM. 2001. Electrically switchable colloidal ordering in confined geometries. *Langmuir* 17:2301–4

Gonzàlez A, Ramos A, Green NG, Castellanos A, Morgan H. 2000. Fluid flow induced by nonuniform ac electric fields in electrolytes on microelectrodes. II. A linear double layer analysis. *Phys. Rev. E* 61:4019–28

Green NG, Ramos A, Gonzàlez A, Morgan H, Castellanos A. 2000. Fluid flow induced by nonuniform ac electric fields in electrolytes on microelectrodes. I. Experimental measurements. *Phys. Rev. E* 61:4011–18

Griffiths SK, Nilson RH. 2000. Band spreading in two-dimensional microchannel turns for electrokinetic species transport. *Anal. Chem.* 72:5473–82

Groisman A, Steinberg V. 2001. Efficient mixing at low Reynolds numbers using polymer additives. *Nature* 410:905–8

Happel J, Brenner H. 1965. *Low Reynolds Number Hydrodynamics*. Englewood Cliffs, NJ: Prentice-Hall. 553 pp.

Herr AE, Molho JI, Santiago JG, Mungal MG,

Kenny TW, Garguilo MG. 2000. Electroosmotic capillary flow with nonniform zeta potential. *Anal. Chem.* 72:1053–57

Ho C-M, Tai Y-C. 1998. Micro-electro-mechanical systems (MEMS) and fluid flows. *Annu. Rev. Fluid Mech.* 30:579–612

Huh D, Tung Y-C, Wei H-H, Grotberg JB, Skerlos SJ, et al. 2002. Use of air-liquid two-phase flow in hydrophobic microfluidic channels for disposable flow cytometers. *Biomed. Microdevices* 4:141–49

Ismagilov RF, Stroock AD, Kenis PJA, Whitesides GM, Stone HA. 2000. Experimental and theoretical scaling laws for transverse diffusive broadening in two-phase laminar flow in microchannels. *Appl. Phys. Lett.* 76:2376–78

Jain KK. 2000. Biochips and microarrays: Technology and commercial potential. *Informa Pharm. Ind. Rep.* London: Informa Pharmaceuticals

Jansons KM. 1988. Determination of the macroscopic (partial) slip boundary condition for a viscous flow over a randomly rough surface with a perfect slip microscopic boundary condition. *Phys. Fluids* 31:15–17

Jendrejack RM, Dimalanta ET, Schwartz DC, Graham MD, de Pablo JJ. 2003. DNA dynamics in a microchannel. *Phys. Rev. Lett.* 91:038102

Johnson RD, Badr IHA, Barrett G, Lai S, Lu Y, et al. 2001. Development of a fully integrated analysis system for ions based on ion-selective optodes and centrifugal microfluidics. *Anal. Chem.* 73:3940–46

Johnson TJ, Locascio LE. 2002. Characterization and optimization of slanted well designs for microfluidic mixing under electroosmotic flow. *Lab Chip* 2:135–40

Johnson TJ, Ross D, Gaitan M, Locascio LE. 2001. Laser modification of preformed polymer microchannels: Application to reduce band broadening around turns subject to electrokinetic flow. *Anal. Chem.* 73:3656–61

Johnson TJ, Ross D, Locascio LE. 2002. Rapid microfluidic mixing. *Anal. Chem.* 74:45–51

Jones SW, Thomas OM, Aref H. 1989. Chaotic advection by laminar flow in a twisted pipe. *J. Fluid Mech.* 209:335–57

Juncker D, Schmid H, Drechsler Wolf H, Michel B, et al. 2002. Microfluidic capillary systems for the autonomous transport of bio/chemicals. *Micro Total Analysis Systems 2002*, ed. Y Baba, S Shoji, A van den Berg, 2:952–54. Dordrecht: Kluwer

Kataoka DE, Troian SM. 1999. Patterning liquid flow on the microscopic scale. *Nature* 402:794–97

Keely CA, Van de Goor TA, McManigill D. 1994. Modeling flow profiles and dispersion in capillary electrophoresis with nonuniform zeta potential. *Anal. Chem.* 66:4236–42

Kenis PJA, Ismagilov RF, Whitesides GM. 1999. Microfabrication inside capillaries using multiphase laminar flow patterning. *Science* 285:83–85

Kim J, Kim C-J. 2002. Nanostructured surfaces for dramatic reduction of flow resistance in droplet-based microfluidics. *Proc. IEEE Conf. MEMS* (Las Vegas, NV) pp. 479–82

Knight JB, Vishwanath A, Brody JP, Austin RH. 1998. Hydrodynamic focusing on a silicon chip: Mixing nanoliters in microseconds. *Phys. Rev. Lett.* 80:3863–66

Kovacs GTA. 1998. *Micromachined Transducers Sourcebook*. Boston: McGraw-Hill. 944 pp.

Kusch H, Ottino JM. 1992. Experiments on mixing in continuous chaotic flows. *J. Fluid Mech.* 236:319–48

Larson RG, Shaqfeh ESG, Muller SJ. 1990. A purely elastic instability in Taylor-Couette flow. *J. Fluid Mech.* 218:573–600

Lauga E, Stone HA. 2003. Effective slip in pressure-driven Stokes flow. *J. Fluid Mech.* 489:55–77

Leal LG. 1992. *Laminar Flow and Convective Transport Processes*. Boston: Butterworth-Heinemann. 740 pp.

Leveque MA. 1928. Les lois de transmission de la chaleur par convection. *Annales de Mines* 13:201–409

Link D, Anna SL, Weitz D, Stone HA. 2003. Geometric mediated breakup of drops in microfluidic devices. Submitted

Liu C, Tai YC, Huang J, Ho CM. 1994. Surface-micromachined thermal shear stress sensor. *Appl. Microfabr. Fluid Mech., ASME* 197:9–16

Liu RH, Stremler MA, Sharp KV, Olsen MG, Santiago JG, et al. 2000. Passive mixing in a three-dimensional serpentine microchannel. *J. Microelectromech. Syst.* 9:190–97

Long D, Stone HA, Ajdari A. 1999. Electroosmotic flows created by surface defects in capillary electrophoresis. *J. Colloid Interface Sci.* 212:338–49

Madou MJ. 1997. *Fundamentals of Microfabrication: The Science of Miniaturization*. Boca Raton, FL: CRC Press. 752 pp.

Martin M, Blu G, Eon C, Guiochon G. 1975. The use of syringe-type pumps in liquid chromatography in order to achieve a constant flow rate. *J. Chromatogr.* 112:399–414

Mazouchi A, Homsy GM. 2001. Thermocapillary migration of long bubbles in polygonal tubes. I. Theory. *Phys. Fluids* 13:1594–1600

Meunier P, Villermaux E. 2003. How vortices mix. *J. Fluid Mech.* 476:213–22

Miyazaki S, Kawai T, Araragi M. 1991. A piezoelectric pump driven by a flexural progressive wave. *Proc. IEEE Micro Electro Mechanical Systems*, pp. 283–88. New York: IEEE

Molho JI, Herr AE, Mosier BP, Santiago JG, Kenny TW, Brennen RA, et al. 2001. Optimization of turn geometries for microchip electrophoresis. *Anal. Chem.* 73:1350–60

Moorthy J, Khoury C, Moore JS, Beebe DJ. 2001. Active control of electroosmotic flow in microchannels using light. *Sens. Actuator B* 75:223–29

Moroney RM, White RM, Howe RT. 1991. Ultrasonically induced microtransport. *Proc. IEEE MEMS, Nara, Jpn.*, pp. 277–82. New York: IEEE

Nadal F, Argoul F, Kestener P, Pouligny B, Ybert C, Ajdari A. 2002. Electrically-induced flows in the vicinity of a dielectric stripe on a conducting plane. *Eur. Phys. J. E* 9:387–99

Ng JMK, Gitlin I, Stroock AD, Whitesides GM. 2002. Components for integrated poly(dimethylsiloxane) microfluidic systems. *Electrophoresis* 23:3461–73

Oddy MH, Santiago JG, Mikkelson JC. 2001. Electrokinetic instability micromixing. *Anal. Chem.* 73:5822–32

Olsson A, Stemme G, Stemme E. 1996. Diffuser-element design investigation for valveless pumps. *Sensors Actuators A* 57:137–43

Ottino JM. 1989. *The Kinematics of Mixing*. Cambridge, UK: Cambridge Univ. Press. 364 pp.

Ottino JM. 1990. Mixing, chaotic advection and turbulence. *Annu. Rev. Fluid Mech.* 22:207–53

Paegel BM, Hutt LD, Simpson PC, Mathies RA. 2000. Turn geometry for minimizing band broadening in microfabricated capillary electrophoresis channels. *Anal. Chem.* 72:3030–3037

Pakdel P, McKinley GH. 1996. Elastic instability and curved streamlines. *Phys. Rev. Lett.* 77:2459–62

Paul PH, Garguilo MG, Rakestraw DJ. 1998. Imaging of pressure and electrokinetically driven flows through open capillaries. *Anal. Chem.* 70:2459–67

Phillips CG. 1990. Heat and mass transfer from a film into steady shear flow. *Q. J. Mech. Appl. Math.* 43:135–59

Pit R, Hervet H, Leger L. 2000. Direct experimental evidence of slip in hexadecane: Solid interfaces. *Phys. Rev. Lett.* 85:980–83

Pollack L, Tate MW, Darnton NC, Knight JB, Gruner SM, et al. 1999. Compactness of the denatured state of a fast-folding protein measured by submillisecond small-angle x-ray scattering. *Proc. Natl. Acad. Sci. USA* 96:10115–17

Pollack MG, Fair RB, Shenderov AD. 2000. Electrowetting-based actuation of liquid droplets for microfluidic applications. *Appl. Phys. Lett.* 77:1725–26

Prins MWJ, Welters WJJ, Weekamp JW. 2001. Fluid control in multichannel structures by electrocapillary pressure. *Science* 291:277–80

Probstein RF. 1994. *Physicochemical Hydrodynamics*. New York: Wiley. 416 pp.

Quake SR, Scherer A. 2000. From micro- to nanofabrication with soft materials. *Science* 290:1536–40

Rallison JR. 1984. The deformation of small viscous drops and bubbles in shear flows. *Annu. Rev. Fluid Mech.* 16:45–66

Ramos A, Morgan H, Green NG, Castellanos A. 1998. AC Electrokinetics: A review of forces in microelectrode structures. *J. Phys. D* 31:2338–53

Ramsey JM, Alarie JP, Jacobson SC, Peterson NJ. 2002. Molecular transport through nanometer confined channels. *Micro Total Analysis 2002*, ed. Y Baba, S Shoji, A van den Berg, 1:314–16. Dordrecht: Kluwer

Ratulowski J, Chang H-C. 1990. Marangoni effects of trace impurities on the motion of long gas bubbles in capillaries. *J. Fluid Mech.* 210:303–28

Ren LQ, Qu WL, Li DQ. 2001. Interfacial electrokinetic effects on liquid flow in microchannels. *Int. J. Heat Mass Transf.* 44: 3125–34

Reyes DR, Iossifidis D, Auroux P-A, Manz A. 2002. Micro total analysis systems. 1. Introduction, theory and technology. *Anal. Chem.* 74:2623–36

Rice CL, Whitehead R. 1965. Electrokinetic flow in a narrow cylindrical capillary. *J. Phys. Chem.* 69:4017–23

Richardson S. 1973. On the no-slip boundary condition. *J. Fluid Mech.* 59:707–19

Russel WB, Saville DA, Schowalter WR. 1989. *Colloidal Dispersions*. Cambridge, UK: Cambridge Univ. Press. 525 pp.

Sammarco TS, Burns MA. 1999. Thermocapillary pumping of discrete drops in microfabricated analysis devices. *AIChE J.* 45:350–66

Santiago JG, Wereley ST, Meinhart CD, Beebe DJ, Adrian RJ. 1998. A particle image velocimetry system for microfluidics. *Exp. Fluids* 25:316–19

Saville DA. 1977. Electrokinetic effects with small particles. *Annu. Rev. Fluid Mech.* 9:321–37

Sawyers DR, Sen M, Chang H-C. 1998. Heat transfer enhancement in three-dimensional corrugated channel flow. *Int. J. Heat Mass Transf.* 41:3559–73

Schasfoort RBM, Schlautmann S, Hendrikse J, van der Berg A. 1999. Field effect flow control for microfabricated fluidic networks. *Science* 286:942–45

Schultz GA, Corso TN, Prosser SJ, Zhang S. 2000. A fully integrated monolithic microchip electrospray device for mass spectrometry. *Anal. Chem.* 72:4058–63

Selverov KP, Stone HA. 2001. Peristaltically driven channel flows with applications toward micro-mixing. *Phys. Fluids* 13:1837–59

Shaqfeh ESG. 1996. Fully elastic instabilities in viscometric flows. *Annu. Rev. Fluid Mech.* 28:129–85

Sharp KVR, Adrian RJ, Santiago JG, Molho JI. 2001. Liquid flow in microchannels. See Gad-el-Hak 2001.

Shrewsbury PJ, Liepmann D, Muller SJ. 2002. Concentration effects of a biopolymer in a microfluidic device. *Biomed. Microdevices* 4:17–26

Smith JT, Elrassi Z. 1993. Capillary zone electrophoresis of biological substances with fused-silica capillaries having zero or constant electroosmotic flow electrophoresis. *Electrophoresis* 14:396–406

Song H, Tice JD, Ismagilov R. 2003. A microfluidic system for controlling reaction networks in time. *Angew. Chem. Int. Ed.* 42: 768–72

Squires T, Bazant MZ. 2003. Induced-charge electro-osmosis. Submitted

Stone HA. 1989. Heat/mass transfer from surface films to shear flows at arbitrary Peclet numbers. *Phys. Fluids* 1:1112–22

Stone HA. 1994. Dynamics of drop deformation and breakup in viscous fluids. *Annu. Rev. Fluid Mech.* 26:65–102

Stone HA, Kim S. 2001. Microfluidics: Basic issues, applications, and challenges. *AIChE J.* 47:1250–54

Stroock AD, Dertinger SKW, Ajdari A, Mezic I, Stone HA, Whitesides GM. 2002a. Chaotic mixer for microchannels. *Science* 295:647–51

Stroock AD, Dertinger SKW, Ajdari A, Whitesides GM. 2002b. Patterning flows using grooved surfaces. *Anal. Chem.* 74:5306–12

Stroock AD, Weck M, Chiu DT, Huck WTS, Kenis PJA, et al. 2000. Patterning electroosmotic flow with patterned surface charge. *Phys. Rev. Lett.* 84:3314–17. Erratum. 2001. *Phys. Rev. Lett.* 86:6050

Studer V, Pépin A, Chen Y, Ajdari A. 2002. Fabrication of microfluidic devices for AC electrokinetic fluid pumping. *Microelectron. Eng.* 61–62:915–20

Sugiura S, Nakajima M, Seki M. 2001. Interfacial tension driven mondispersed droplet formation from microfabricated channel array. *Langmuir* 17:5562–66

Tabeling P. 2001. Some basic problems of microfluidics. *14th Aust. Fluid Mech. Conf., Univ. Adelaide*

Tai YC, Muller RS. 1988. Lightly-doped polysilicon bridge as a flow meter. *Sensors Actuators* 15:63–75

Takayama S, Ostuni E, LeDuc P, Naruse K, Ingber DE, Whitesides GM. 2001. Laminar flows: Subcellular positioning of small molecules. *Nature* 411:1016

Takhistov P, Indeikina A, Chang H-C. 2002. Electrokinetic displacement of air bubbles in microchannels. *Phys. Fluids* 14:1–14

Taylor GI. 1934. The formation of emulsions in definable fields of flow. *Proc. R. Soc. London Ser. A* 146:501–23

Taylor GI. 1953. Dispersion of soluble matter in solvent flowing slowly through a tube. *Proc. R. Soc. London Ser. A* 219:186–203

Thorsen T, Maerkl SJ, Quake SR. 2002. Microfluidic large-scale integration. *Science* 298:580–84

Thorsen T, Roberts RW, Arnold FH, Quake SR. 2001. Dynamic pattern formation in a vesicle-generating microfluidic device. *Phys. Rev. Lett.* 86:4163–66

Trau M, Saville DA, Aksay IA. 1996. Field-induced layering of colloidal crystals. *Science* 272:706–9

Unger MA, Chou H-P, Thorson T, Scherer A, Quake SR. 2000. Monolithic microfabricated valves and pumps by multilayer soft lithography. *Science* 288:113–16

Vinogradova OI. 1999. Slippage of water over hydrophobic surfaces. *Int. J. Miner. Process.* 56:31–60

Voldman J, Gray ML, Schmidt MA. 1999. Microfabrication in biology and medicine. *Annu. Rev. Biomed. Eng.* 1:401–25

Ward T, Homsy GM. 2001. Electrohydrodynamically driven chaotic mixing in a translating drop. *Phys. Fluids* 13:3521–25

Weigl BH, Yager P. 1999. Microfluidic diffusion-based separation and detection. *Science* 283:346–47

Whitesides GM, Stroock AD. 2001. Flexible methods for microfluidics. *Phys. Today* 54:42–48

Wong H, Radke CJ, Morris S. 1995a. The motion of long bubbles in polygonal capillaries: I. Thin films. *J. Fluid Mech.* 292:71–94

Wong H, Radke CJ, Morris S. 1995b. The motion of long bubbles in polygonal capillaries: II. Drag, fluid pressure, and fluid flow. *J. Fluid Mech.* 292:95–110

Yeh SR, Seul M, Shraiman BI. 1997. Assembly of ordered colloidal aggregates by electric-field induced fluid-flow. *Nature* 386:57–59

Yi MQ, Bau HH, Hu H. 2002a. Peristaltically induced motion in a closed cavity with two vibrating walls. *Phys. Fluids* 14:184–97

Yi MQ, Qian SZ, Bau HH. 2002b. A magnetohydrodynamic chaotic stirrer. *J. Fluid Mech.* 468:153–77

Zabow G, Assi F, Jenks R, Prentiss M. 2002. Guided microfluidics by electromagnetic capillary focusing. *Appl. Phys. Lett.* 80:1483–85

Zhao B, Moore JS, Beebe DJ. 2001. Surface-directed liquid flow inside microchannels. *Science* 291:1023–26

Zhu YX, Granick S. 2002. Limits of the hydrodynamic no-slip boundary condition. *Phys. Rev. Lett.* 88:106102

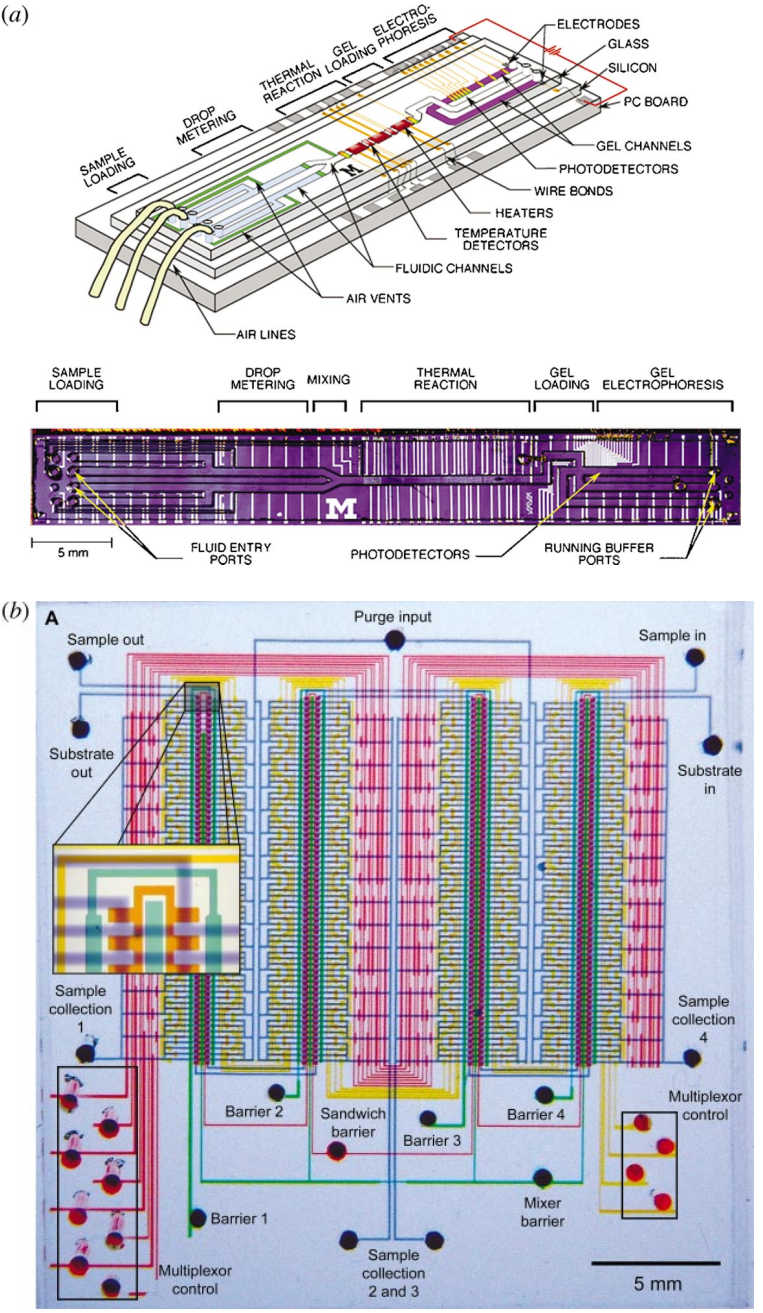

See legend on next page

Figure 1 (*a*) A lab-on-a-chip aims to reduce in scale all of the elements of the chemical and processing worlds. This scaling down involves flow and transport necessary for multiple chemical analyses, mixing, detection, separation, and so on. The "chip" shown here was described by Burns et al. 1998. (*b*) Optical micrograph of a microfluidic device containing 2056 channels (Thorsen et al. 2002). The various input chambers contain dye to visualize the structure of the network.

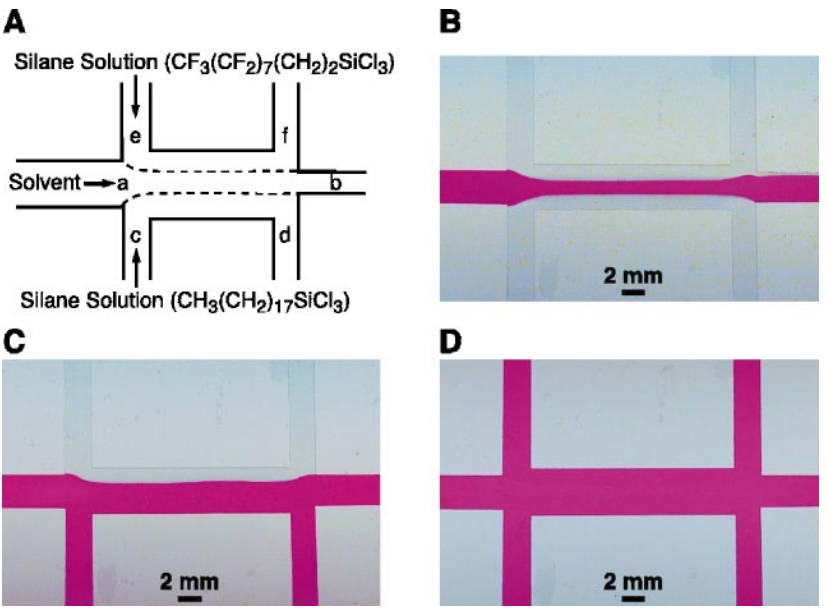

Figure 3 Chemical modifications of a microchannel to control the wettability of a surface for designing pressure-sensitive valves (Zhao et al. 2001). (*A*) Laminar flow is used to make a hydrophilic central stripe surrounded on one side by an OTS monolayer and on the other by an HFTS monolayer. (*B*) With a low driving pressure, (dyed) water is confined to the central channel. As the driving force is increased, first the lower boundary "ruptures" (*C*) and at even higher pressure (*D*) both boundaries rupture.

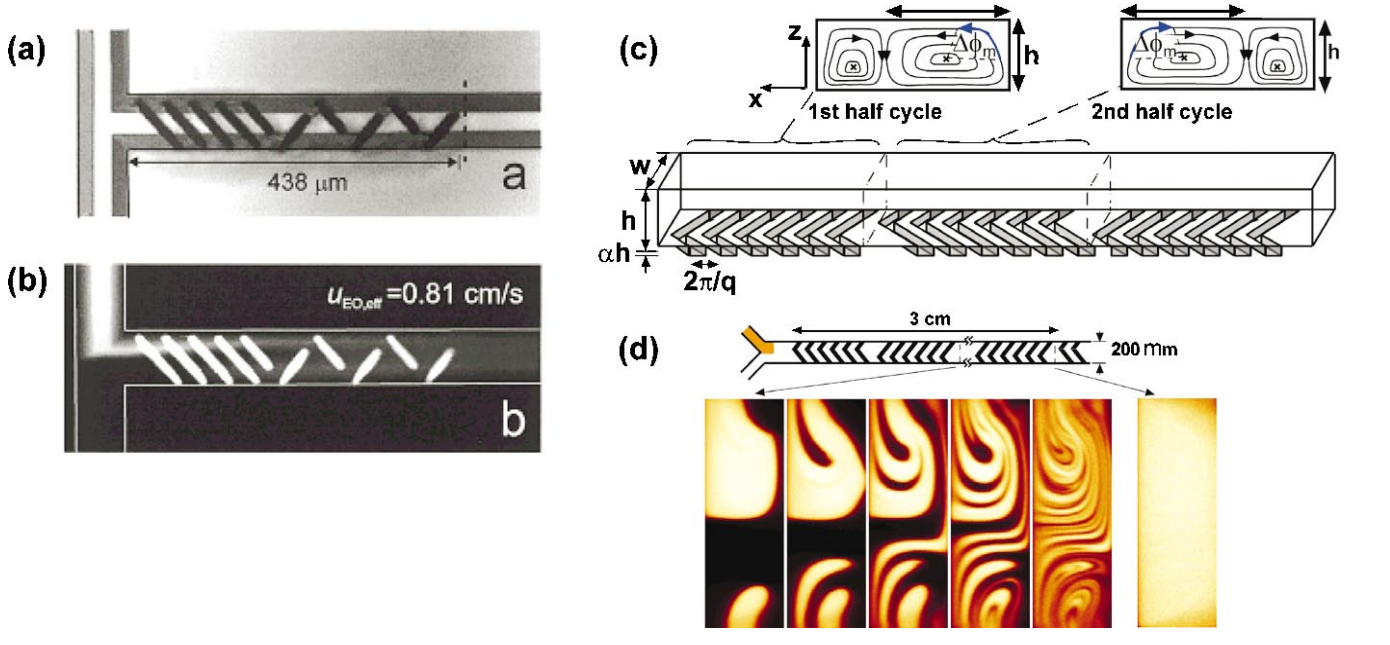

Figure 6 Passive micromixers for EOF and pressure-driven flows based on obliquely oriented grooves. (*a*) Optical micrograph showing the top view of a channel for electro-osmotic flows (Johnson et al. 2002). The diagonal lines are grooves on the floor of the channel. (*b*) Fluorescence micrograph of a stream of fluorescent solution being mixed with a nonfluorescent solution in the same channel as in (*a*). (*c*) Schematic diagram of a section of a microchannel with surface grooves for mixing with pressure-driven flows (Stroock et al. 2002a). One and a half cycles of the mixing pattern are shown. Above the channel, the streamlines of the average flow in the cross section are shown schematically for each half-cycle. (*d*) A mixing experiment with equal streams of fluorescent and nonfluorescent solutions in a channel, as in (*c*). The confocal images show the progress after each of the first five cycles, and after 15 cycles (≈3 cm downstream).

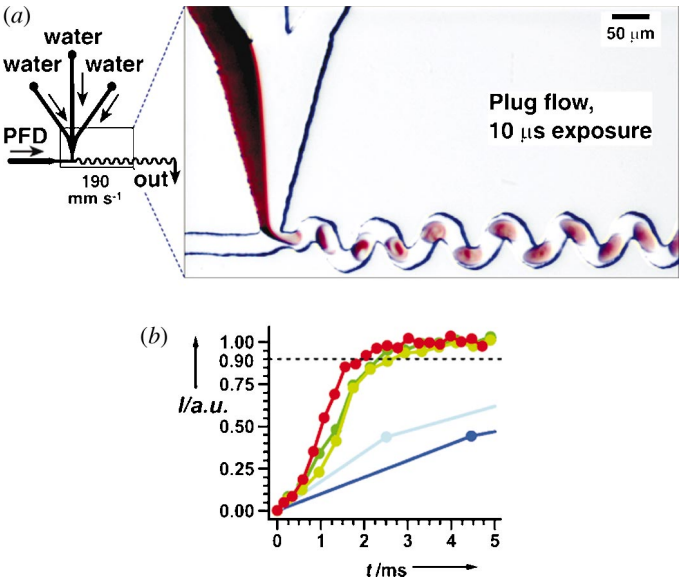

Figure 7 Drops as small mixing chambers with the rate of mixing enhanced by motion in a wavy channel (Song et al. 2003). (*a*) Microphotographs with 10-μs exposure illustrating rapid mixing inside water drops in a continuous phase of perfluorodecalinee (PFD). (*b*) In experiments similar to (*a*) a fast chemical reaction utilizing a fluorescent marker is used from which the relative normalized intensity of the fluorescence signal is obtained as a function of travel time for flow rates (dark blue toward red) 10, 19, 190, 190, and 300 mm/s. All channels are 45 μm deep, inlet channels are 50 μm wide, and the curved channel is 29 μm wide.

Annual Review of Fluid Mechanics
Volume 36, 2004

CONTENTS